

# Experimental studies of the $\eta'$ -nucleus interaction in photonuclear reactions

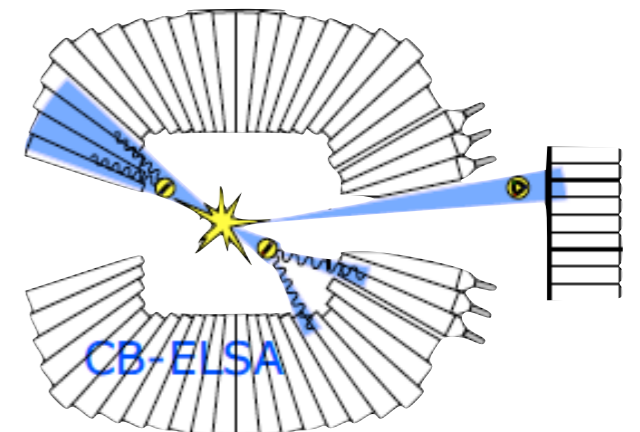
Mariana Nanova, Volker Metag

II. Physikalisches Institut



## outline

- introduction
- scattering length
- complex meson-nucleus potentials
- theoretical predictions
- experimental approaches
- experimental results on the  $\eta'$ -nucleus potential
- search for  $\eta'$  mesic states
- summary and conclusion



# Introduction: bound systems

---

earth ↔ moon



bound by gravitation

# Introduction: bound systems

---

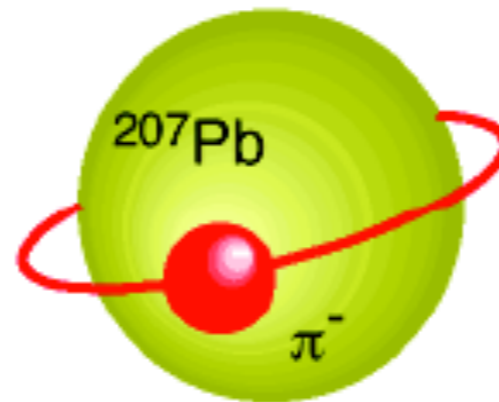
earth  $\leftrightarrow$  moon



bound by gravitation

**charged meson**

$\pi^- \leftrightarrow$  nucleus



bound by superposition  
of attractive Coulomb-  
and repulsive strong  
interaction

talk by Kenta Itahashi

# Introduction: bound systems

---

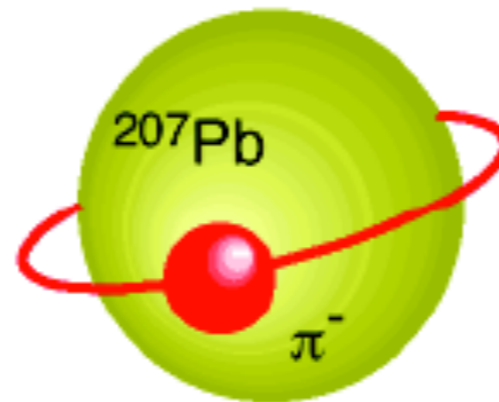
earth  $\leftrightarrow$  moon



bound by gravitation

**charged meson**

$\pi^- \leftrightarrow$  nucleus

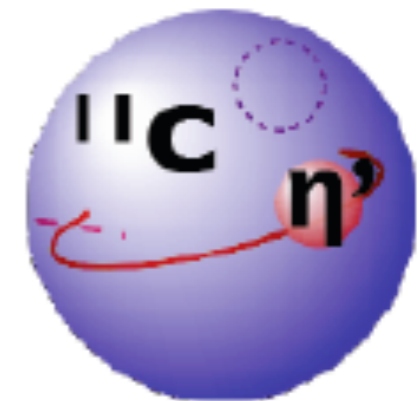


bound by superposition  
of attractive Coulomb-  
and repulsive strong  
interaction

talk by Kenta Itahashi

**neutral meson**

$\omega, \eta' \leftrightarrow$  nucleus

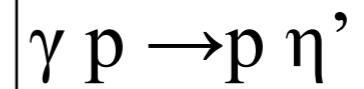
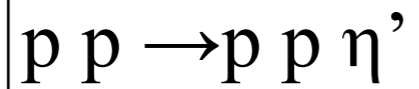


bound solely by  
the strong interaction



talk by Yoshiki Tanaka

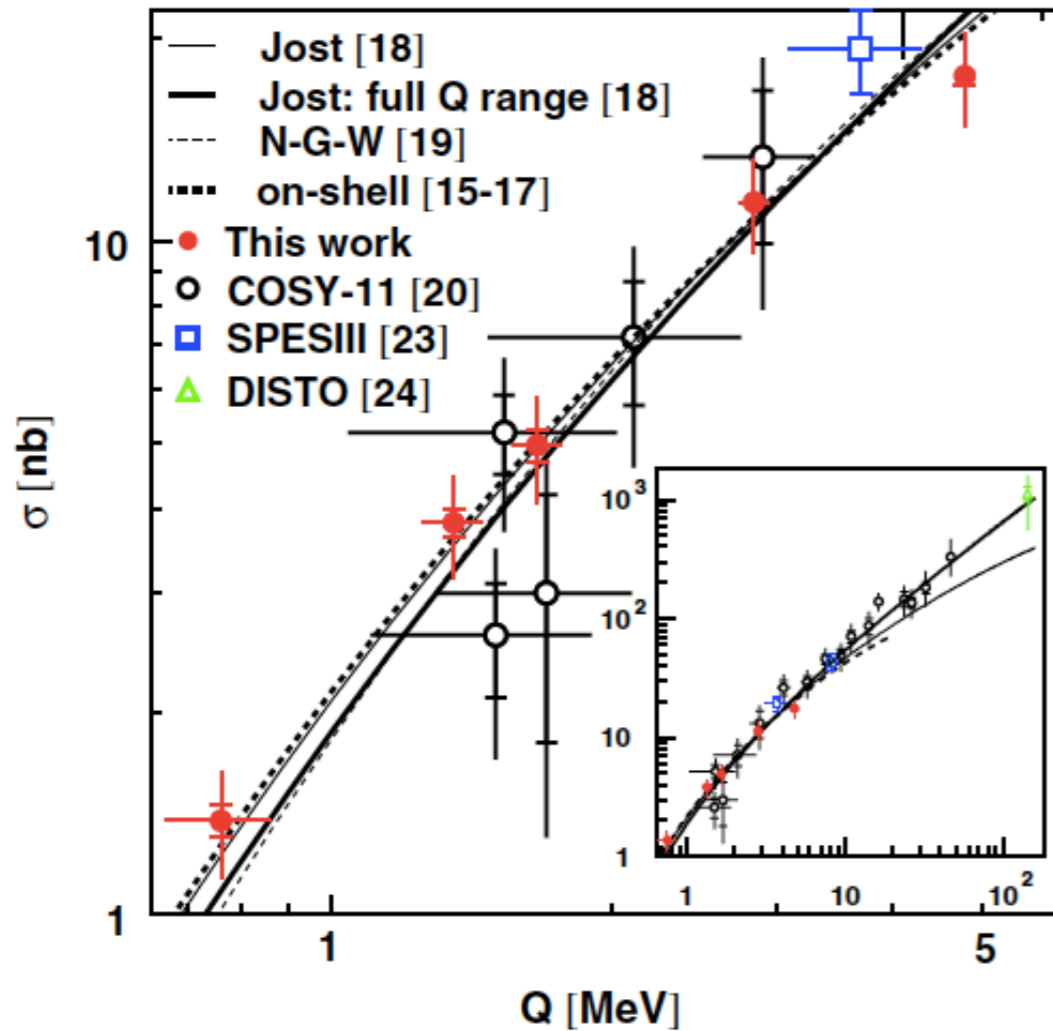
# Determinations of the $\eta'$ scattering length



near threshold measurement!!!

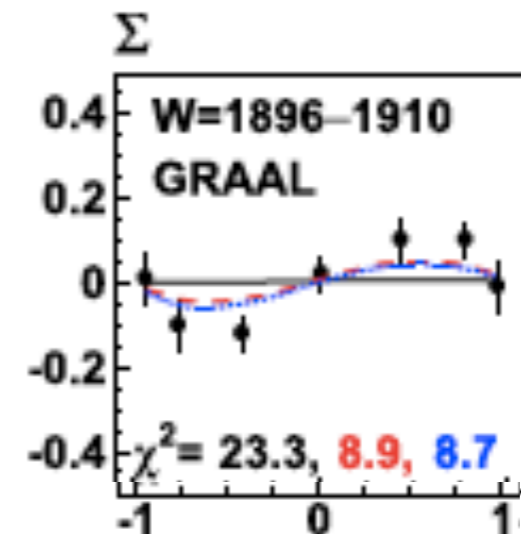
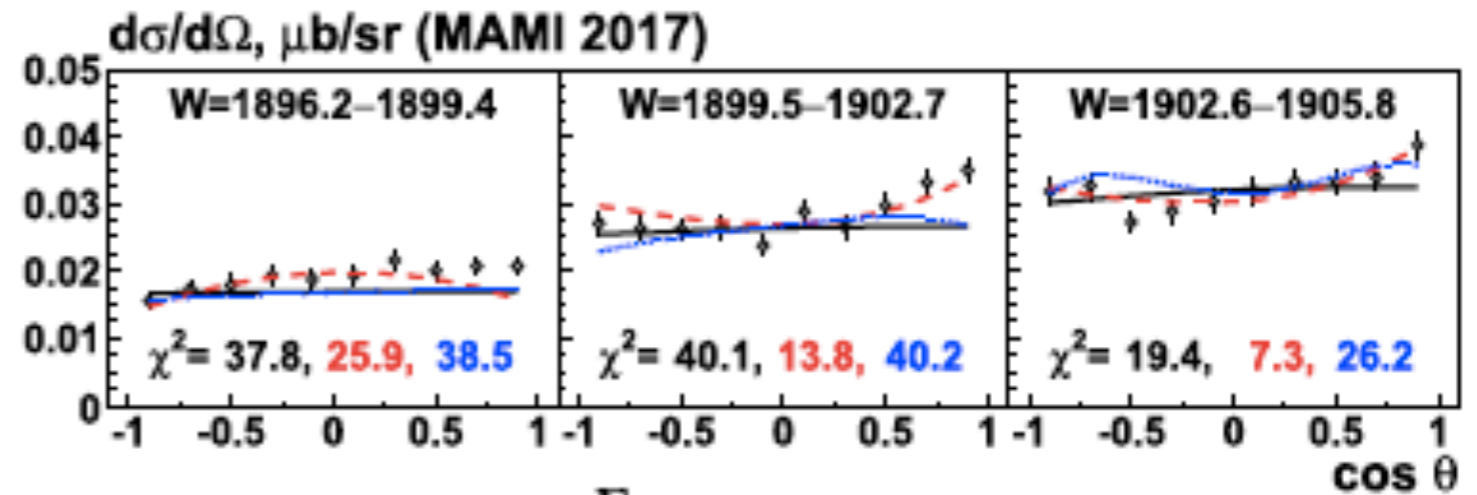
E. Czerwinski et al., PRL 113 (2014) 062004

A. V. Anisovich et al. PLB 785 (2018) 626



$$a_{\eta'p} = (0 \pm 0.43) + i(0.37_{-0.16}^{+0.40}) \text{ fm}$$

$$|a_{\eta'p}| = 0.37_{-0.46}^{+0.59} \text{ fm}$$

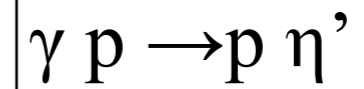
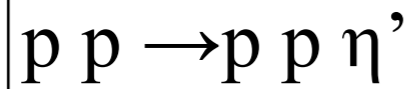


$$|a_{\eta'p}| = 0.403 \pm 0.015 \pm 0.06 \text{ fm}$$

$$\delta_{\eta'p} = (87 \pm 2)^{\circ}$$



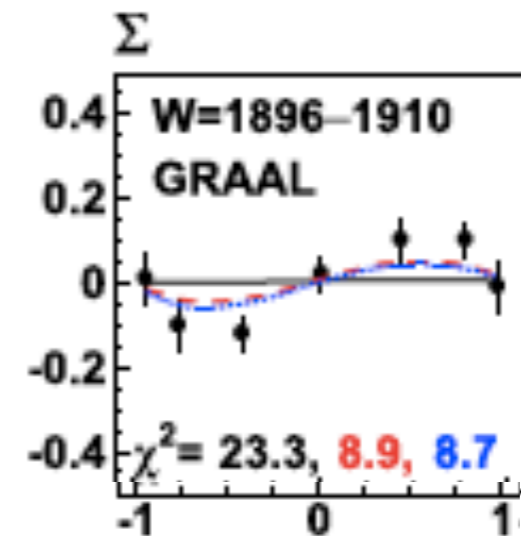
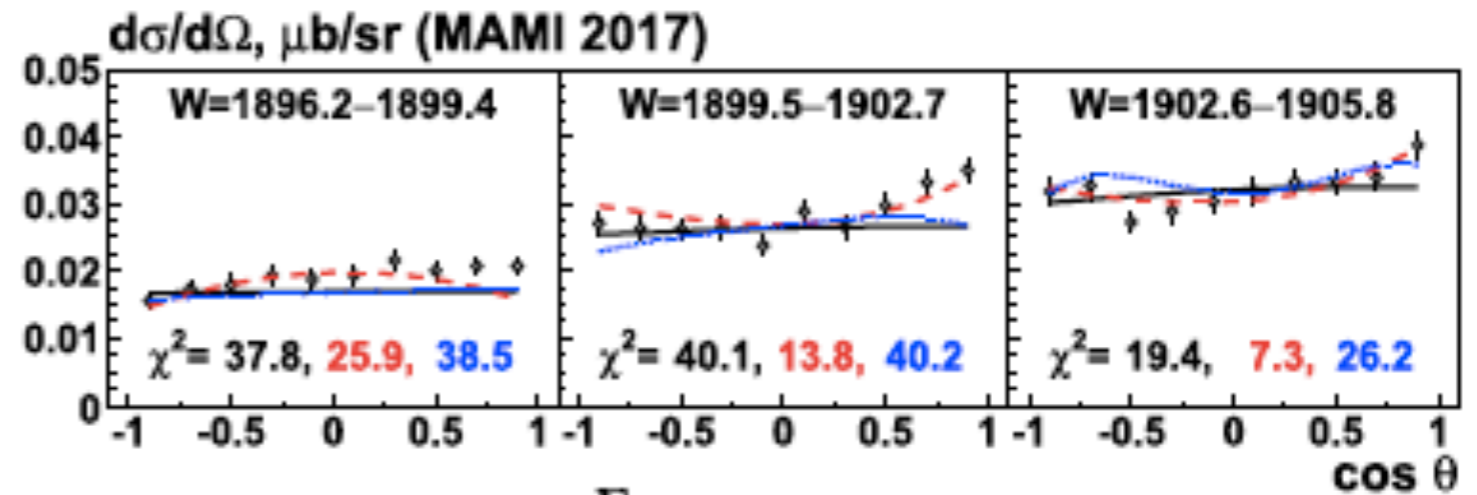
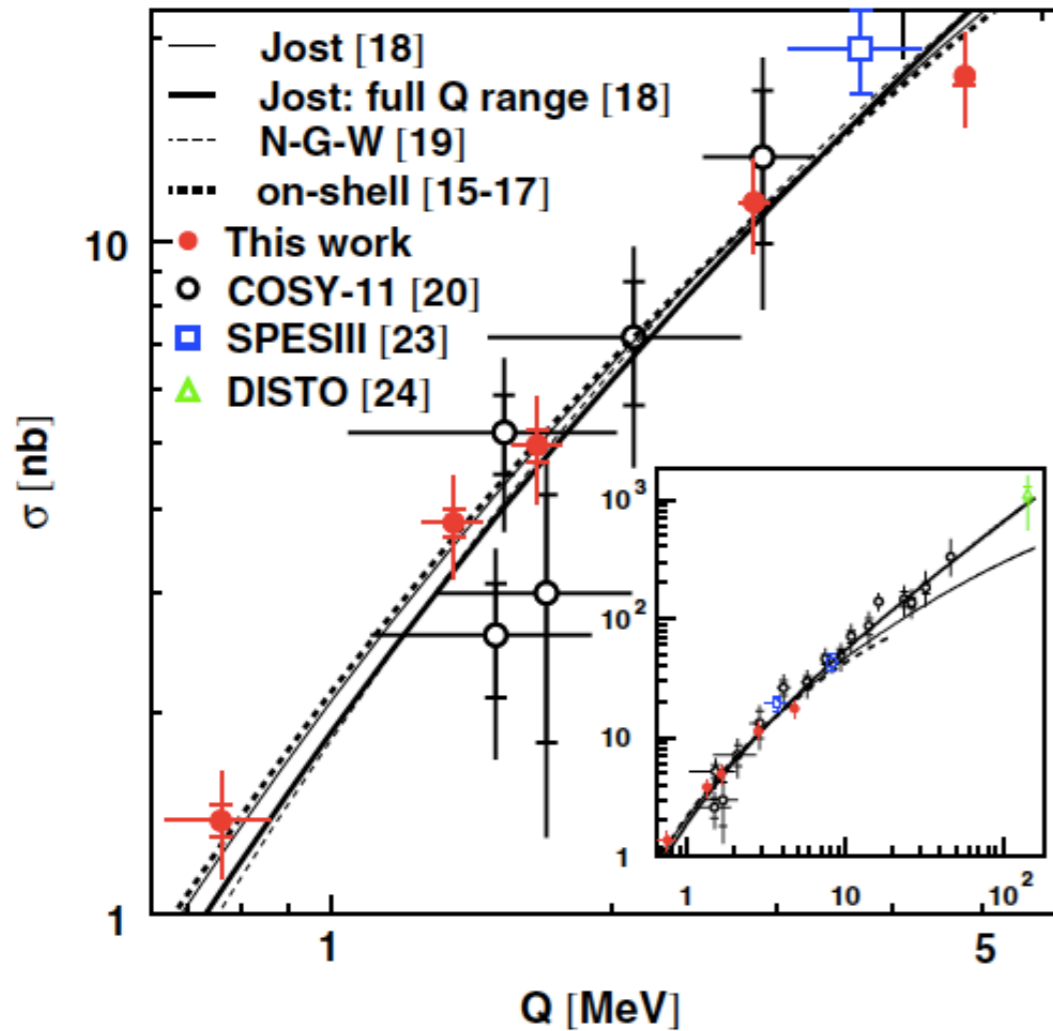
# Determinations of the $\eta'$ scattering length



near threshold measurement!!!

E. Czerwinski et al., PRL 113 (2014) 062004

A. V. Anisovich et al. PLB 785 (2018) 626



$$a_{\eta'p} = (0 \pm 0.43) + i(0.37_{-0.16}^{+0.40}) \text{ fm}$$

$$|a_{\eta'p}| = 0.403 \pm 0.015 \pm 0.06 \text{ fm}$$

$$|a_{\eta'p}| = 0.37_{-0.46}^{+0.59} \text{ fm}$$

$$\delta_{\eta'p} = (87 \pm 2)^{\circ}$$

modulus in agreement !

# Meson-nucleus complex potential

---

H. Nagahiro, S. Hirenzaki, PRL 94 (2005) 232503

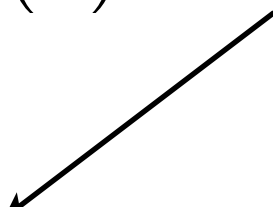
$$U(r) = V(r) + iW(r)$$

# Meson-nucleus complex potential

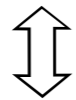
---

H. Nagahiro, S. Hirenzaki, PRL 94 (2005) 232503

$$U(r) = V(r) + iW(r)$$


$$V(r) = \Delta m(\rho_0) \cdot \frac{\rho(r)}{\rho_0}$$

real part



**in-medium mass modification**



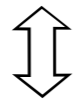
# Meson-nucleus complex potential

H. Nagahiro, S. Hirenzaki, PRL 94 (2005) 232503

$$U(r) = V(r) + iW(r)$$

$$V(r) = \Delta m(\rho_0) \cdot \frac{\rho(r)}{\rho_0}$$

real part



**in-medium mass modification**

$$W(r) = -\Gamma_0/2 \cdot \frac{\rho(r)}{\rho_0} \\ = -\frac{1}{2} \cdot \hbar c \cdot \rho(r) \cdot \sigma_{inel} \cdot \beta$$

imaginary part



**lifetime shortened**  
in-medium width  
inelastic cross section

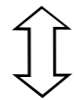
# Meson-nucleus complex potential

H. Nagahiro, S. Hirenzaki, PRL 94 (2005) 232503

$$U(r) = V(r) + iW(r)$$

$$V(r) = \Delta m(\rho_0) \cdot \frac{\rho(r)}{\rho_0}$$

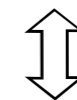
real part



**in-medium mass modification**

$$W(r) = -\Gamma_0/2 \cdot \frac{\rho(r)}{\rho_0} \\ = -\frac{1}{2} \cdot \hbar c \cdot \rho(r) \cdot \sigma_{inel} \cdot \beta$$

imaginary part



**lifetime shortened**  
in-medium width  
inelastic cross section

**mass and lifetime (width) may be changed in the medium**

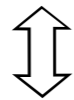
# Meson-nucleus complex potential

H. Nagahiro, S. Hirenzaki, PRL 94 (2005) 232503

$$U(r) = V(r) + iW(r)$$

$$V(r) = \Delta m(\rho_0) \cdot \frac{\rho(r)}{\rho_0}$$

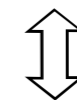
real part



**in-medium mass modification**

$$W(r) = -\Gamma_0/2 \cdot \frac{\rho(r)}{\rho_0} \\ = -\frac{1}{2} \cdot \hbar c \cdot \rho(r) \cdot \sigma_{inel} \cdot \beta$$

imaginary part



**lifetime shortened**  
in-medium width  
inelastic cross section

**mass and lifetime (width) may be changed in the medium**

$\eta'$  -nucleus potential derived from  $\eta'$  - p scattering length

E. Friedman and A. Gal, Phys. Rep. 452 (2007) 89

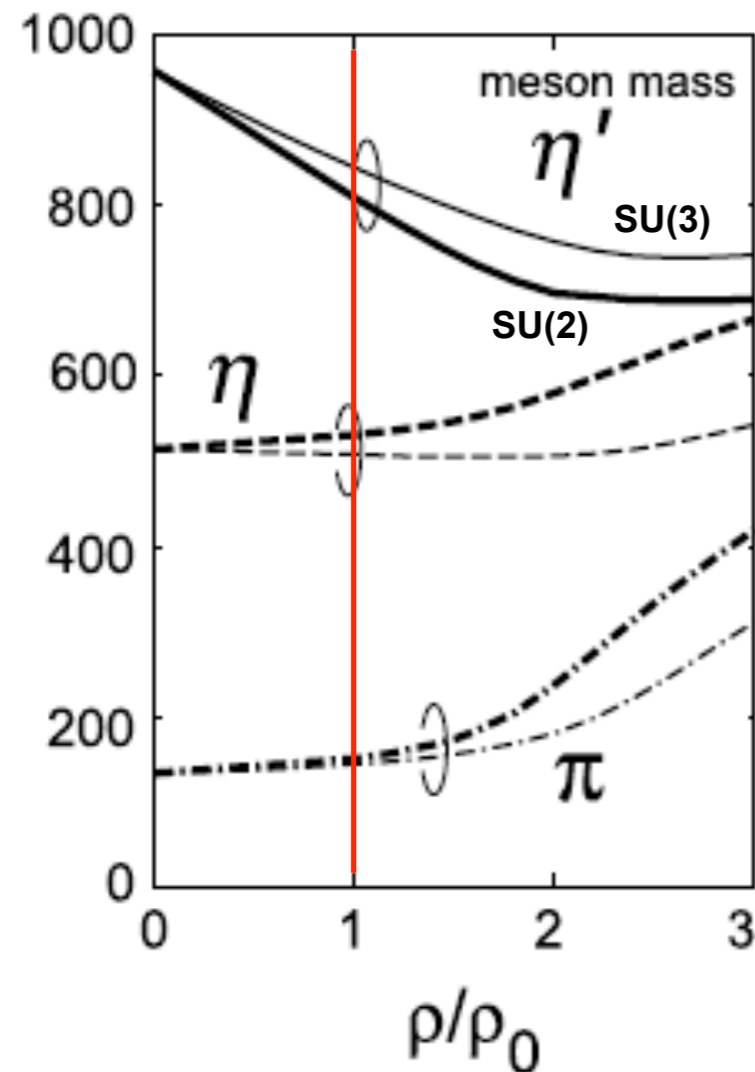
with  $2\mu V_{opt} = -4\pi \left(1 + \frac{A-1}{A} \frac{\mu}{M_N}\right) a \rho \hbar^2$  and  $\mu = \frac{M_{\eta'} \cdot M_A}{M_{\eta'} + M_A}$

$$U_0 = V_0 + i W_0 = -(0 \pm 37.9 + i \cdot 32.6_{-14.1}^{+35.2}) \text{ MeV}$$

# Model predictions for the real part of the $\eta'$ A interaction

## NJL-model

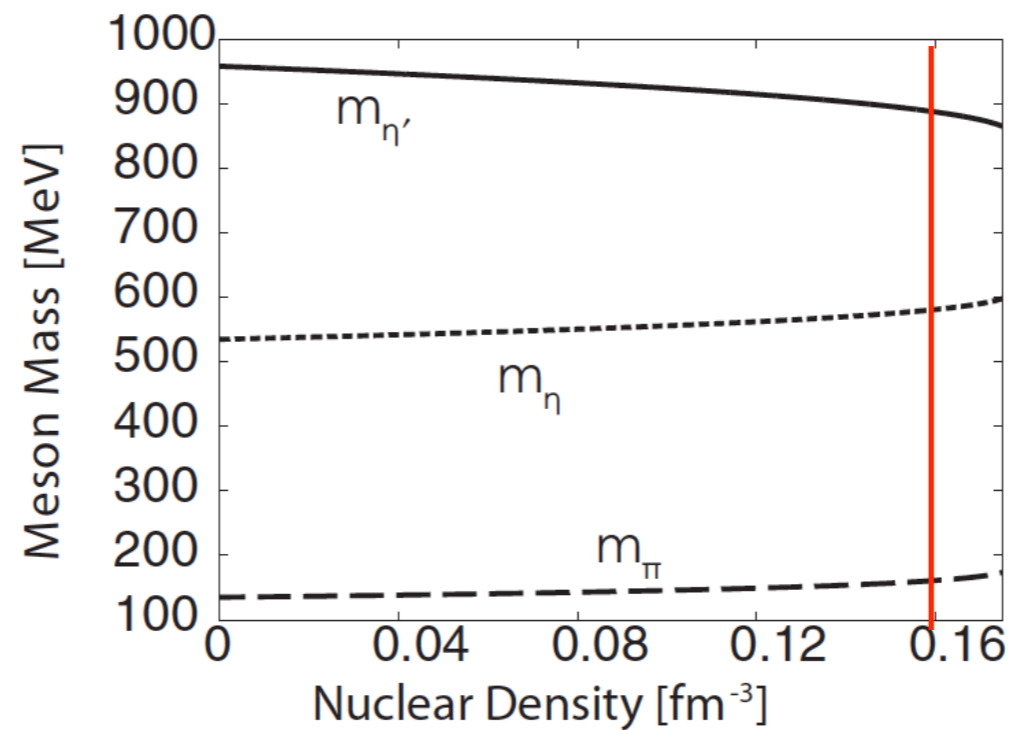
H. Nagahiro, M. Takizawa and S. Hirenzaki,  
Phys. Rev. C 74 (2006) 045203



$\Delta m_{\eta'}(\rho_0) \approx -150$  MeV  
 $\Delta m_{\eta}(\rho_0) \approx +20$  MeV

## linear $\sigma$ model

S. Sakai and D. Jido  
PRC 88 (2013) 064906



$\Delta m_{\eta'}(\rho_0) \approx -80$  MeV

## QMC-model

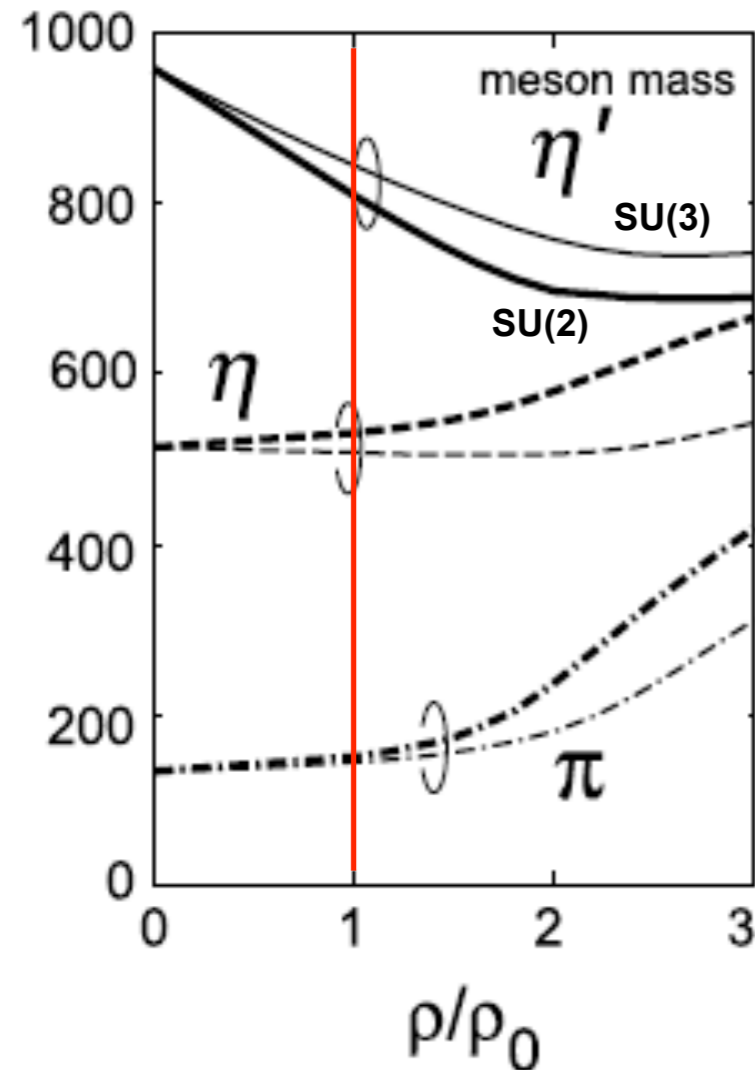
S. Bass and A. Thomas,  
PLB 634 (2006) 368

$\Delta m_{\eta'}(\rho_0) \approx -40$  MeV  
 for  $\theta_{\eta\eta'} = -20^\circ$

# Model predictions for the real part of the $\eta'$ A interaction

## NJL-model

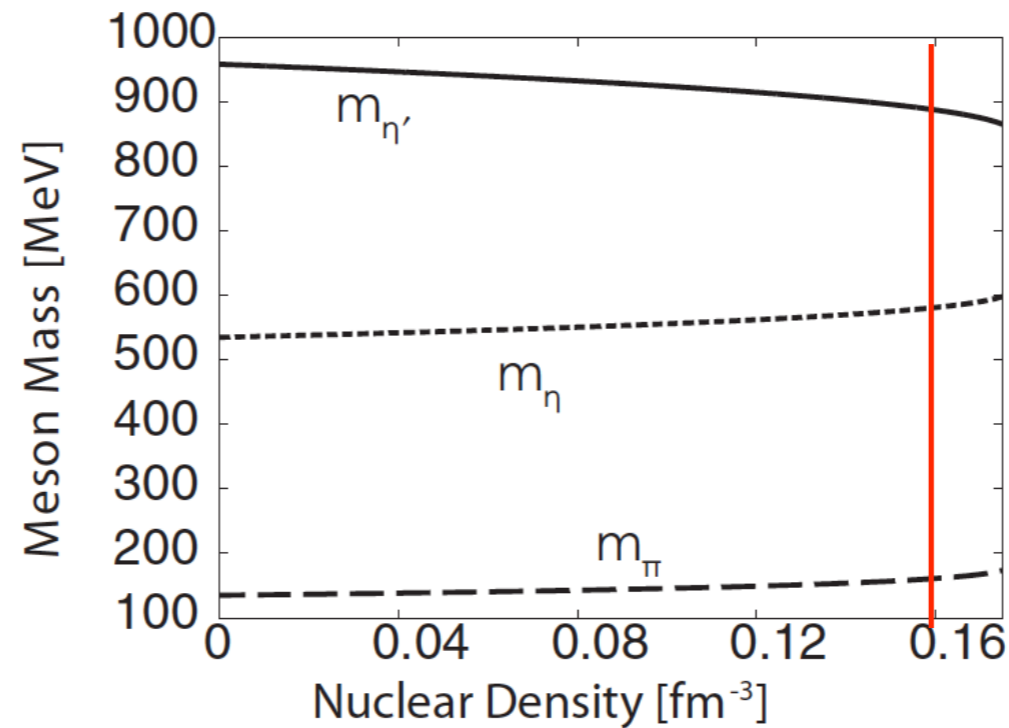
H. Nagahiro, M. Takizawa and S. Hirezaki,  
Phys. Rev. C 74 (2006) 045203



$\Delta m_{\eta'}(\rho_0) \approx -150$  MeV  
 $\Delta m_{\eta}(\rho_0) \approx +20$  MeV

## linear $\sigma$ model

S. Sakai and D. Jido  
PRC 88 (2013) 064906



$\Delta m_{\eta'}(\rho_0) \approx -80$  MeV

## QMC-model

S. Bass and A. Thomas,  
PLB 634 (2006) 368

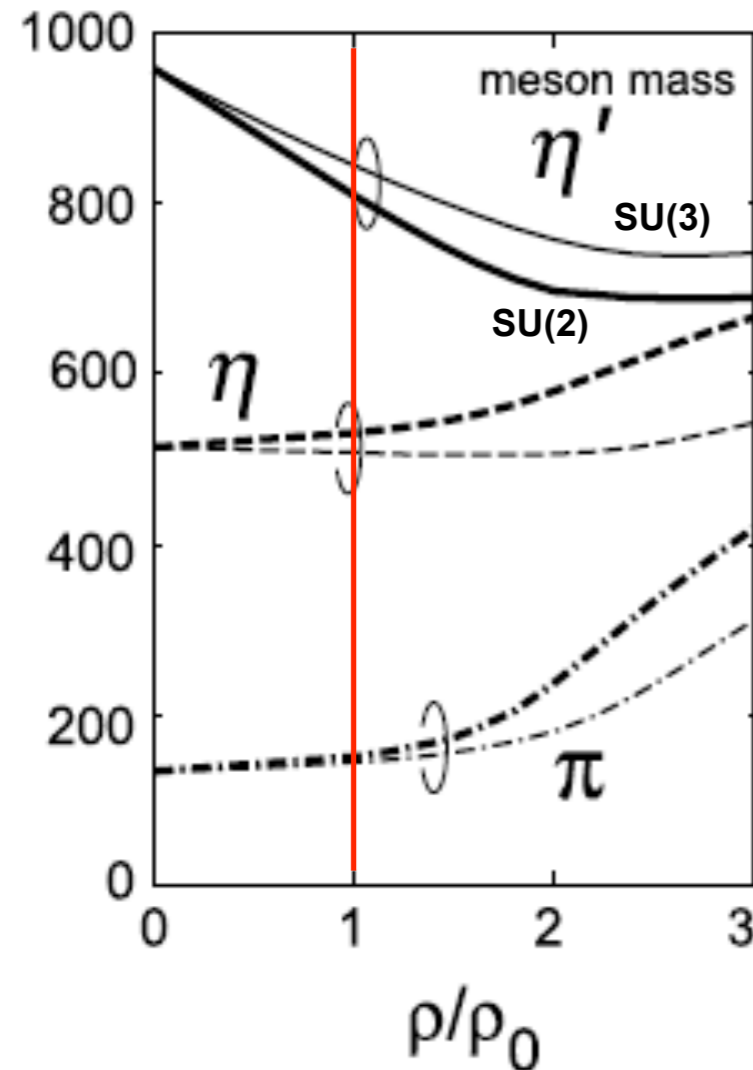
$\Delta m_{\eta'}(\rho_0) \approx -40$  MeV  
 for  $\theta_{\eta\eta'} = -20^\circ$

**throughout  
 attractive potential  
 predicted!  
 in  
 conflict with  $a_{\eta'p}$  ?**

# Model predictions for the real part of the $\eta'$ A interaction

## NJL-model

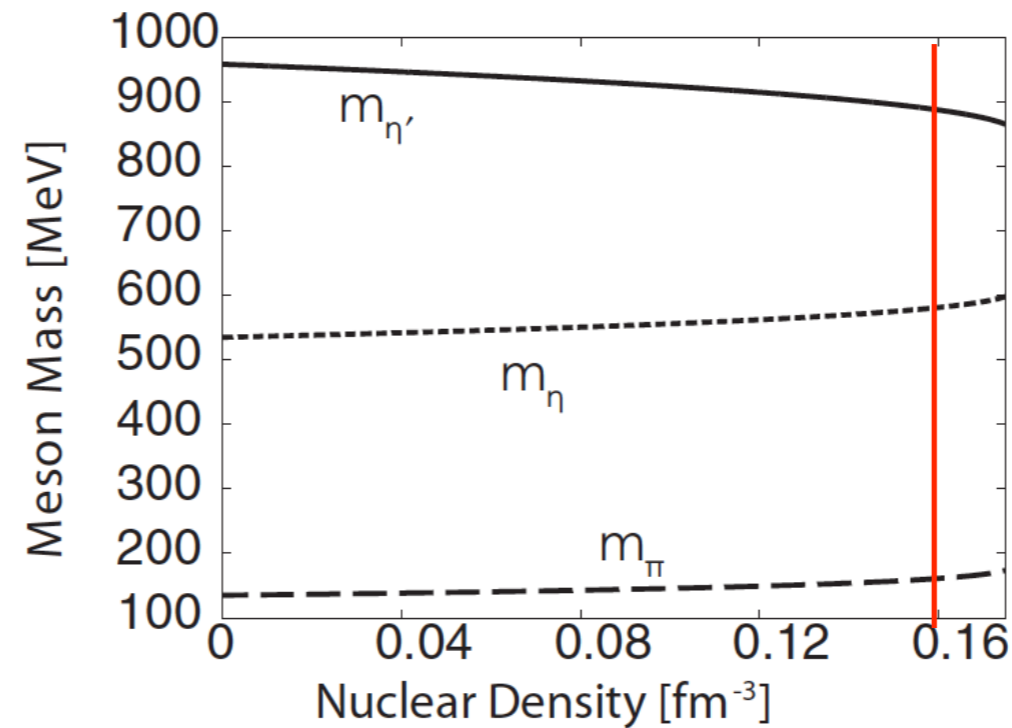
H. Nagahiro, M. Takizawa and S. Hirezaki,  
Phys. Rev. C 74 (2006) 045203



$\Delta m_{\eta'}(\rho_0) \approx -150$  MeV  
 $\Delta m_{\eta}(\rho_0) \approx +20$  MeV

## linear $\sigma$ model

S. Sakai and D. Jido  
PRC 88 (2013) 064906



$\Delta m_{\eta'}(\rho_0) \approx -80$  MeV

## QMC-model

S. Bass and A. Thomas,  
PLB 634 (2006) 368

$\Delta m_{\eta'}(\rho_0) \approx -40$  MeV  
 for  $\theta_{\eta\eta'} = -20^\circ$

**throughout  
 attractive potential  
 predicted!  
 in  
 conflict with  $a_{\eta'p}$  ?**

*experimental clarification needed!*



# From theoretical predictions to experimental observables

---

calculations of meson spectral functions assume:

- infinitely extended nuclear matter in equilibrium at  $\rho$ ,  $T = \text{const.}$ ;
- meson at rest in nuclear medium

# From theoretical predictions to experimental observables

---

calculations of meson spectral functions assume:

- infinitely extended nuclear matter in equilibrium at  $\rho$ ,  $T = \text{const.}$ ;
- meson at rest in nuclear medium

theoretical  
predictions



experimental  
observables

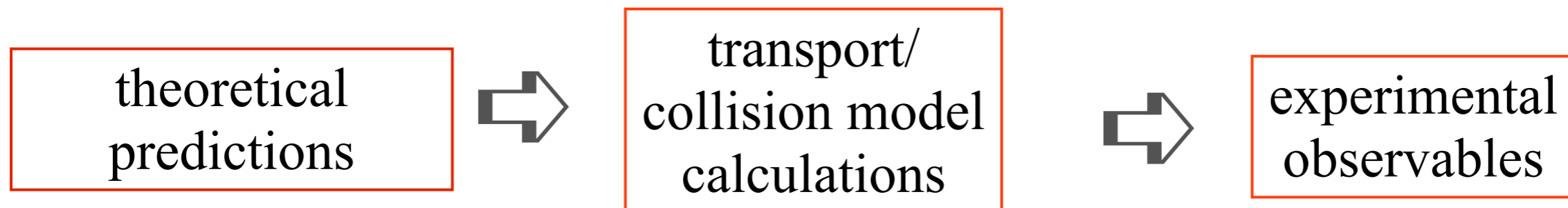
# From theoretical predictions to experimental observables

---

calculations of meson spectral functions assume:

- infinitely extended nuclear matter in equilibrium at  $\rho$ ,  $T = \text{const.}$ ;
- meson at rest in nuclear medium

transport calculations (GiBUU, HSD, UrQMD, JAM,...) or  
collision model calculations  
are needed for comparison with experiment !!!



- initial state effects: absorption of incoming beam particles
- non equilibrium effects: varying density and temperature
- absorption and regeneration of mesons in the nuclear medium
- only fraction of decays inside of the nuclear environment
- final state interactions: distortion of momenta of decay products

# Experimental approaches to determine the meson-nucleus optical potential

---

$$U(r) = V(r) + iW(r)$$

real part



$$V(r) = \Delta m(\rho_0) \cdot \frac{\rho(r)}{\rho_0}$$

- line shape analysis\*
- excitation function
- momentum distribution
- meson-nucleus bound states

# Experimental approaches to determine the meson-nucleus optical potential

---

$$U(r) = V(r) + iW(r)$$

←  
real part

$$V(r) = \Delta m(\rho_0) \cdot \frac{\rho(r)}{\rho_0}$$

- line shape analysis\*
- excitation function
- momentum distribution
- meson-nucleus bound states

\*not applicable;

$\eta'$  meson decays outside of nucleus;

$M_0 = 957.78 \text{ MeV}$  ;  $\Gamma_0 = 0.194 \text{ MeV}$ ;

$\lambda_{dec} = \hbar c / \Gamma_0 = 1000 \text{ fm} \gg \gg R_{nucl}$

# Experimental approaches to determine the meson-nucleus optical potential

$$U(r) = V(r) + iW(r)$$

real part

imaginary part

$$V(r) = \Delta m(\rho_0) \cdot \frac{\rho(r)}{\rho_0}$$

$$W(r) = -\Gamma_0/2 \cdot \frac{\rho(r)}{\rho_0} \\ = -\frac{1}{2} \cdot \hbar c \cdot \rho(r) \cdot \sigma_{inel} \cdot \beta$$

- line shape analysis\*
- excitation function
- momentum distribution
- meson-nucleus bound states

- transparency ratio measurement

$$T_A = \frac{\sigma_{\gamma A \rightarrow \eta' X}}{A \cdot \sigma_{\gamma N \rightarrow \eta' X}}$$

\*not applicable;

$\eta'$  meson decays outside of nucleus;

$M_0 = 957.78 \text{ MeV}$  ;  $\Gamma_0 = 0.194 \text{ MeV}$ ;

$\lambda_{dec} = \hbar c / \Gamma_0 = 1000 \text{ fm} \gg \gg R_{nucl}$

D. Cabrera et al., NPA 733 (2004)130

attenuation measurement

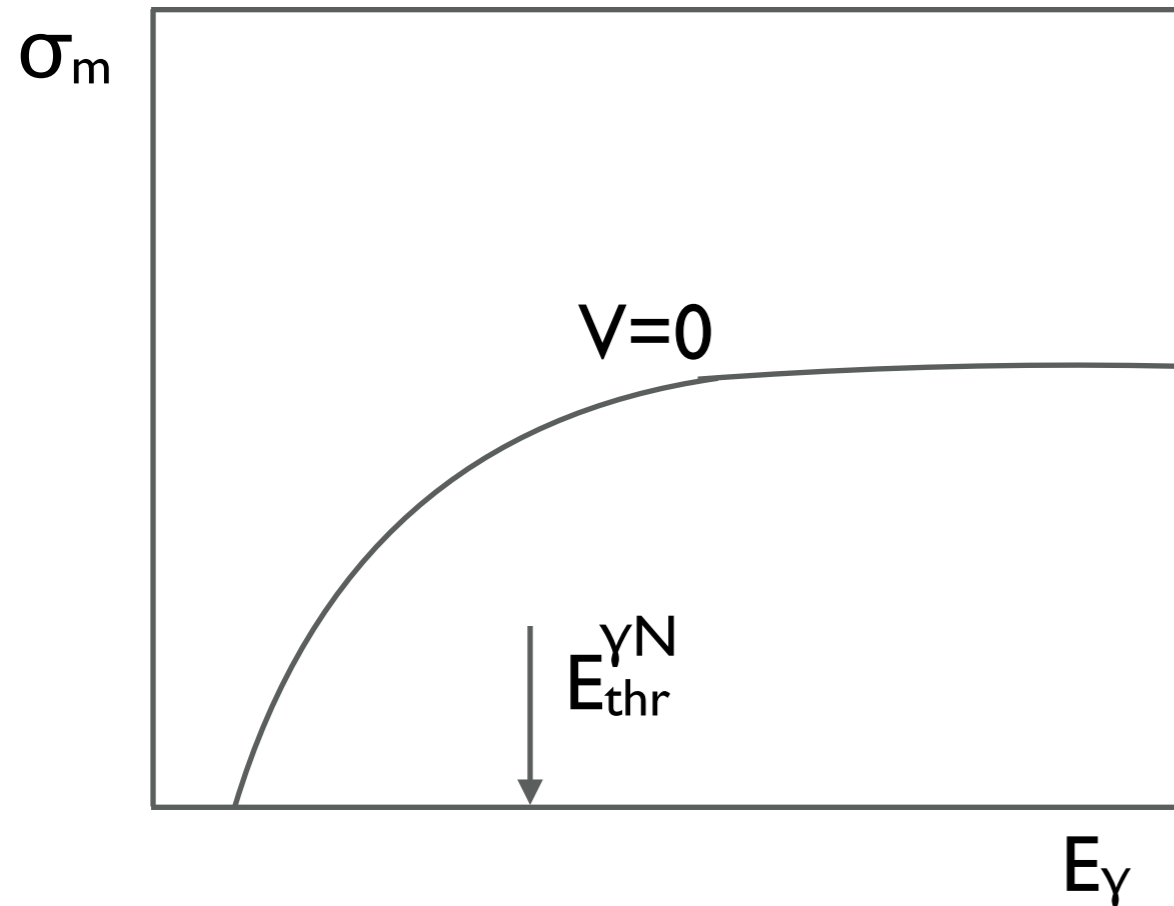
of the  $\eta'$  meson flux



# Determining the real part of the meson-nucleus potential from excitation functions and momentum distributions

sensitive to nuclear density at the **production point**

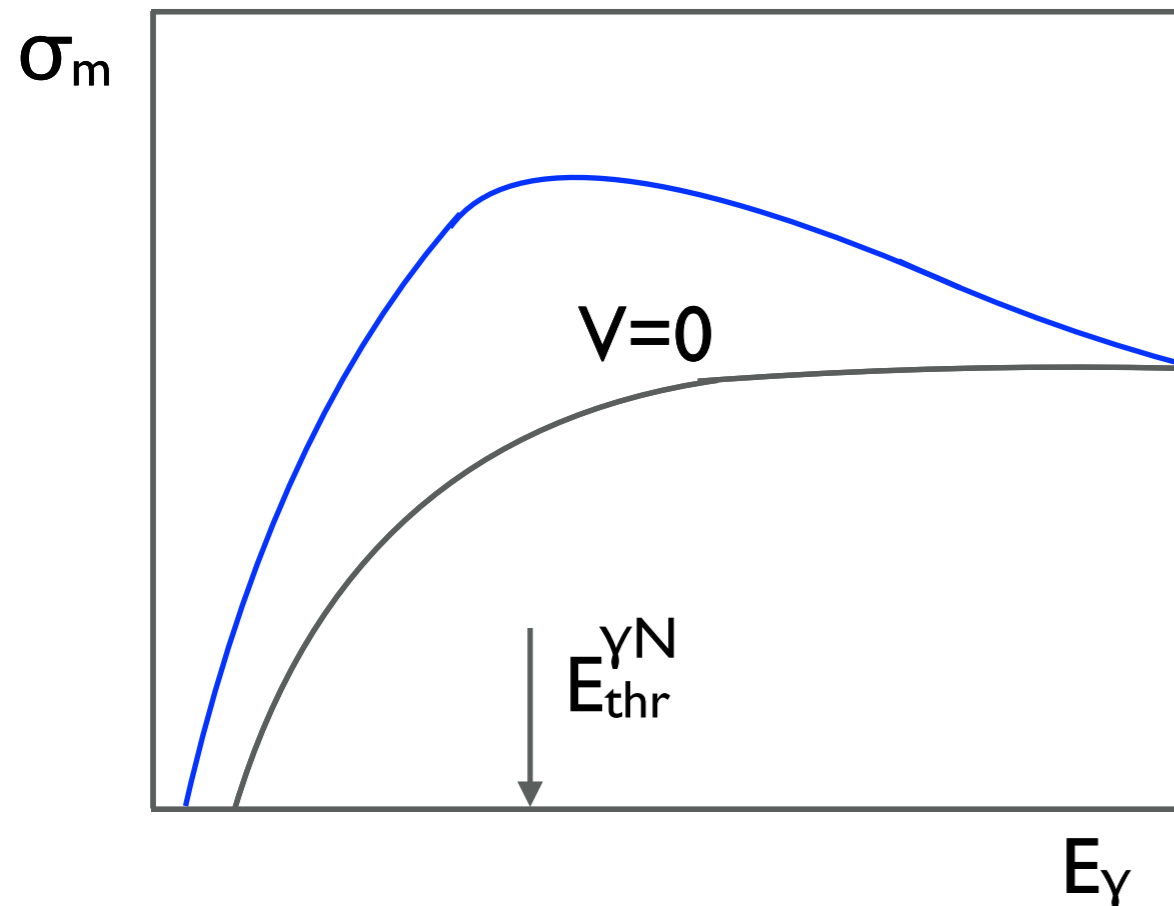
excitation function



# Determining the real part of the meson-nucleus potential from excitation functions and momentum distributions

sensitive to nuclear density at the **production point**

excitation function

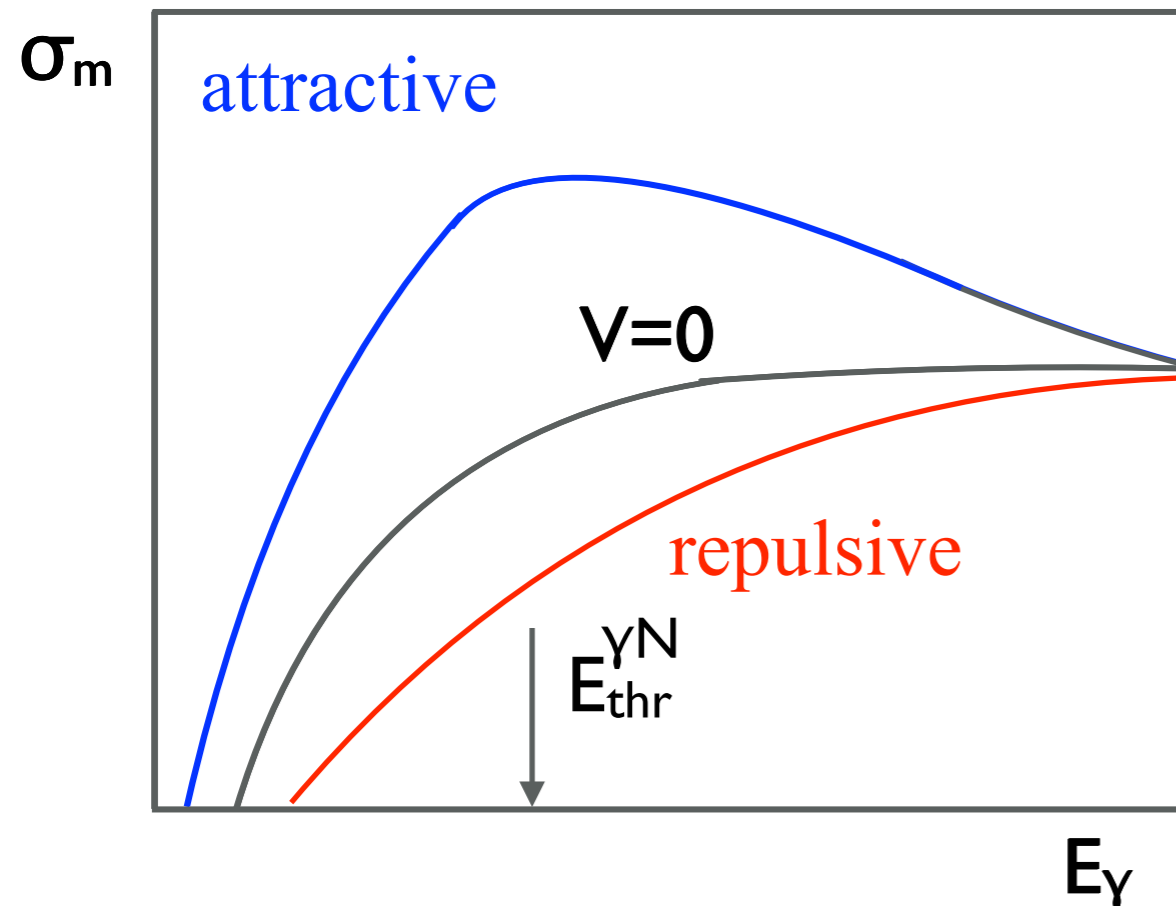


attractive interaction  $\rightarrow$  mass drop  $\rightarrow$   
lower threshold  $\rightarrow$  larger phase space  $\rightarrow$   
larger cross section

# Determining the real part of the meson-nucleus potential from excitation functions and momentum distributions

sensitive to nuclear density at the **production point**

excitation function



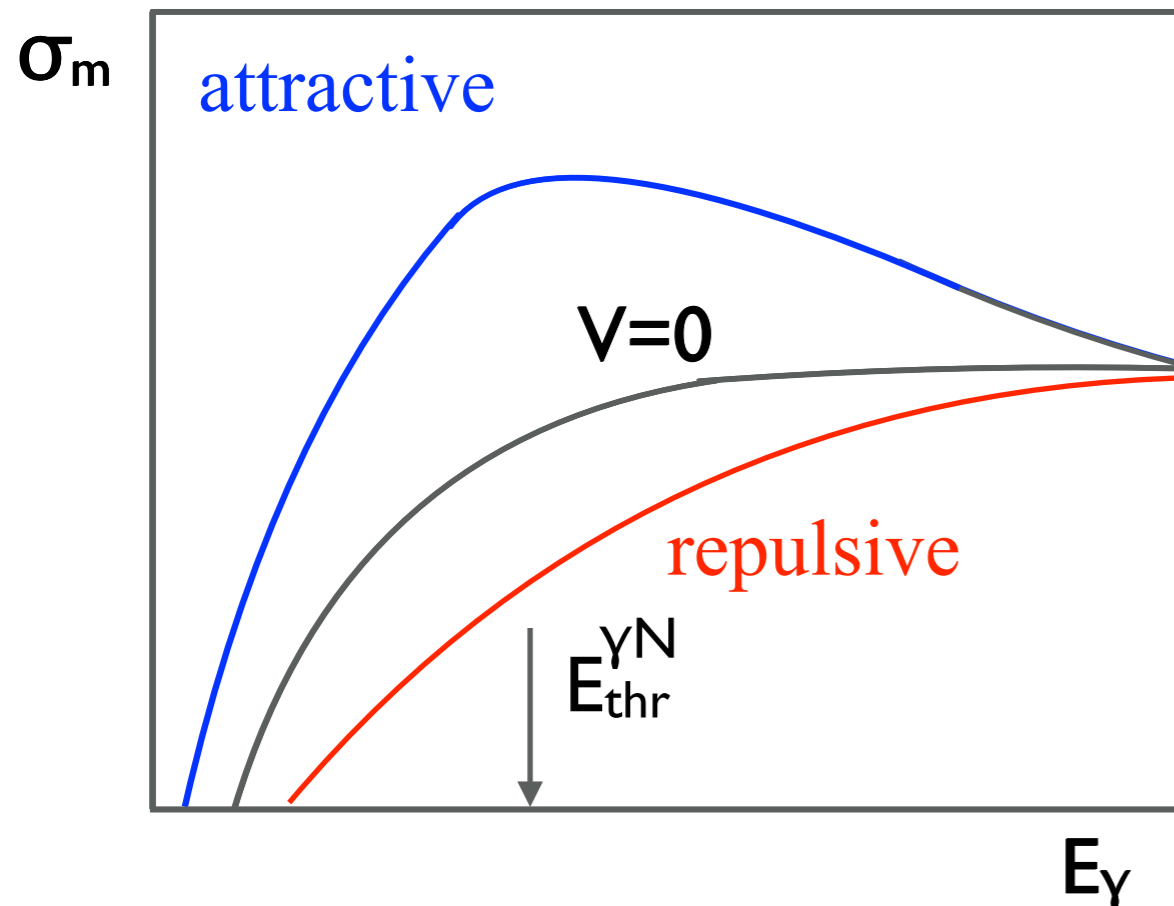
attractive interaction  $\rightarrow$  mass drop  $\rightarrow$   
lower threshold  $\rightarrow$  larger phase space  $\rightarrow$   
larger cross section

repulsive interaction  $\rightarrow$  mass increase  $\rightarrow$   
higher threshold  $\rightarrow$  smaller phase space  $\rightarrow$   
smaller cross section

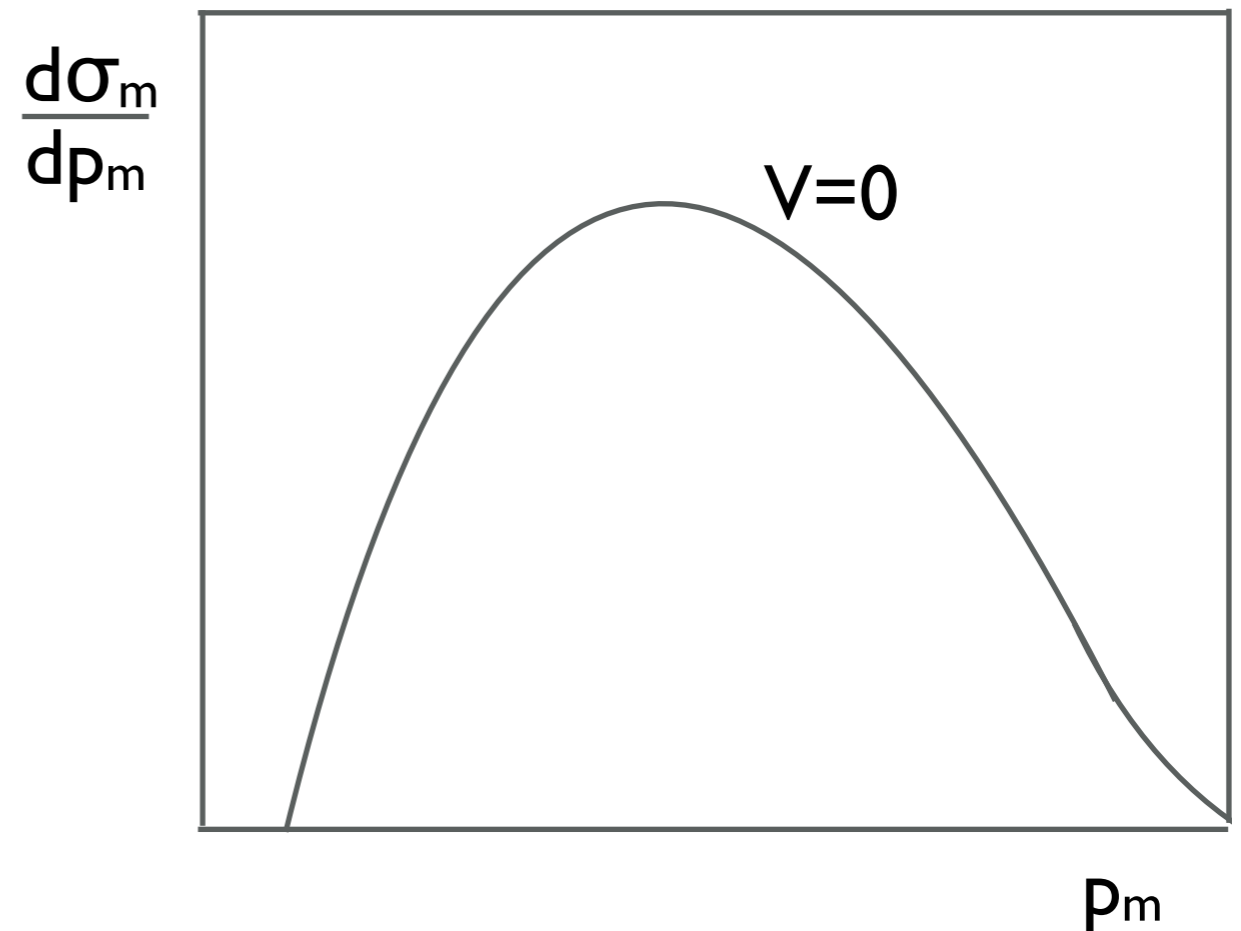
# Determining the real part of the meson-nucleus potential from excitation functions and momentum distributions

sensitive to nuclear density at the **production point**

excitation function



momentum distribution



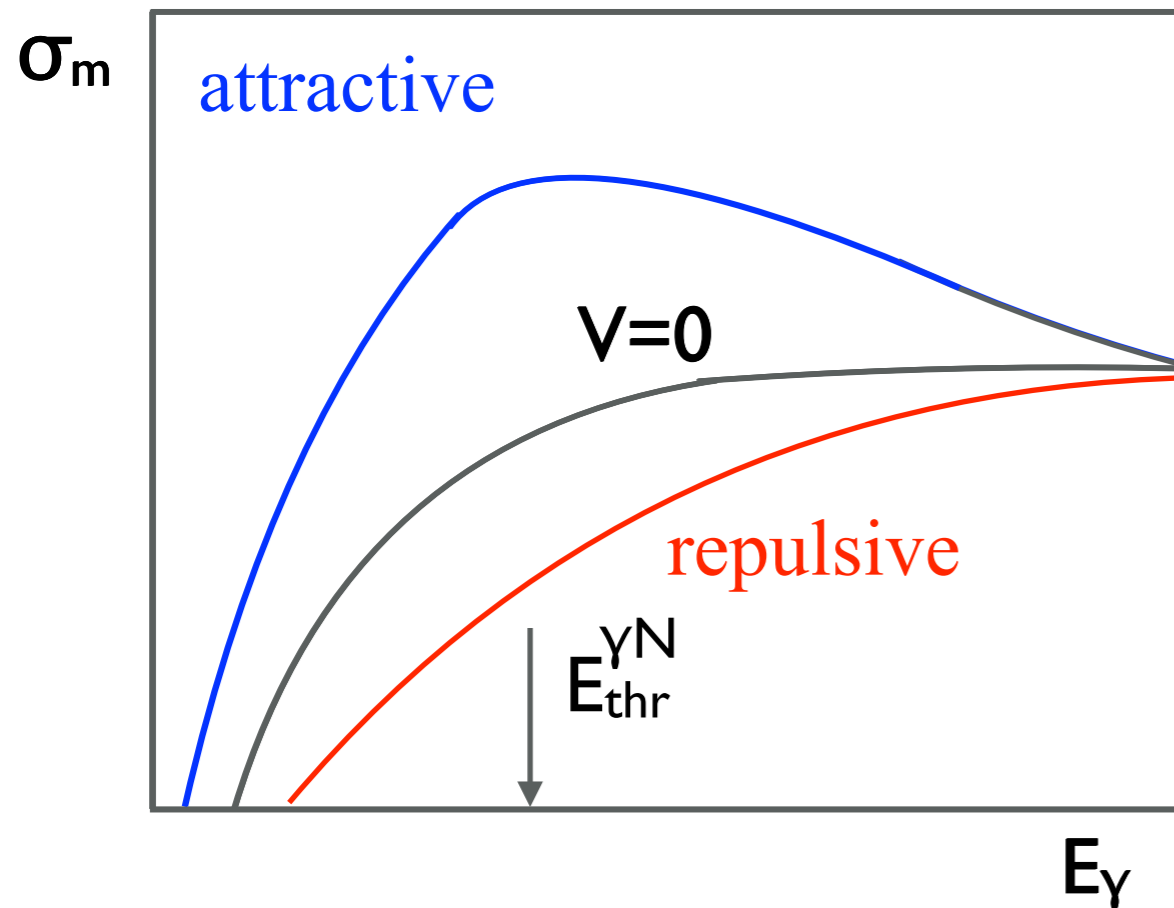
attractive interaction  $\rightarrow$  mass drop  $\rightarrow$   
lower threshold  $\rightarrow$  larger phase space  $\rightarrow$   
larger cross section

repulsive interaction  $\rightarrow$  mass increase  $\rightarrow$   
higher threshold  $\rightarrow$  smaller phase space  $\rightarrow$   
smaller cross section

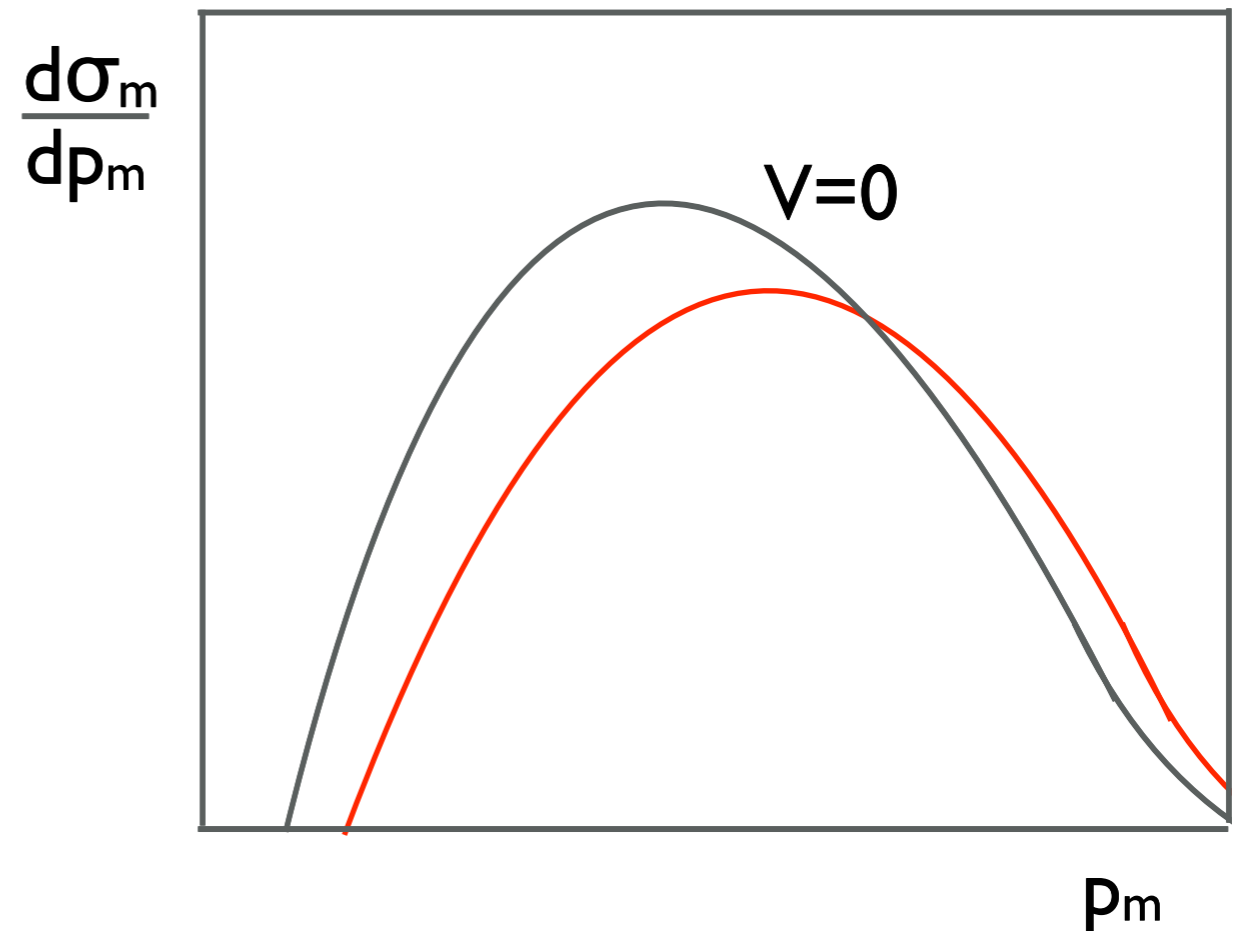
# Determining the real part of the meson-nucleus potential from excitation functions and momentum distributions

sensitive to nuclear density at the **production point**

excitation function



momentum distribution



attractive interaction  $\rightarrow$  mass drop  $\rightarrow$   
lower threshold  $\rightarrow$  larger phase space  $\rightarrow$   
larger cross section

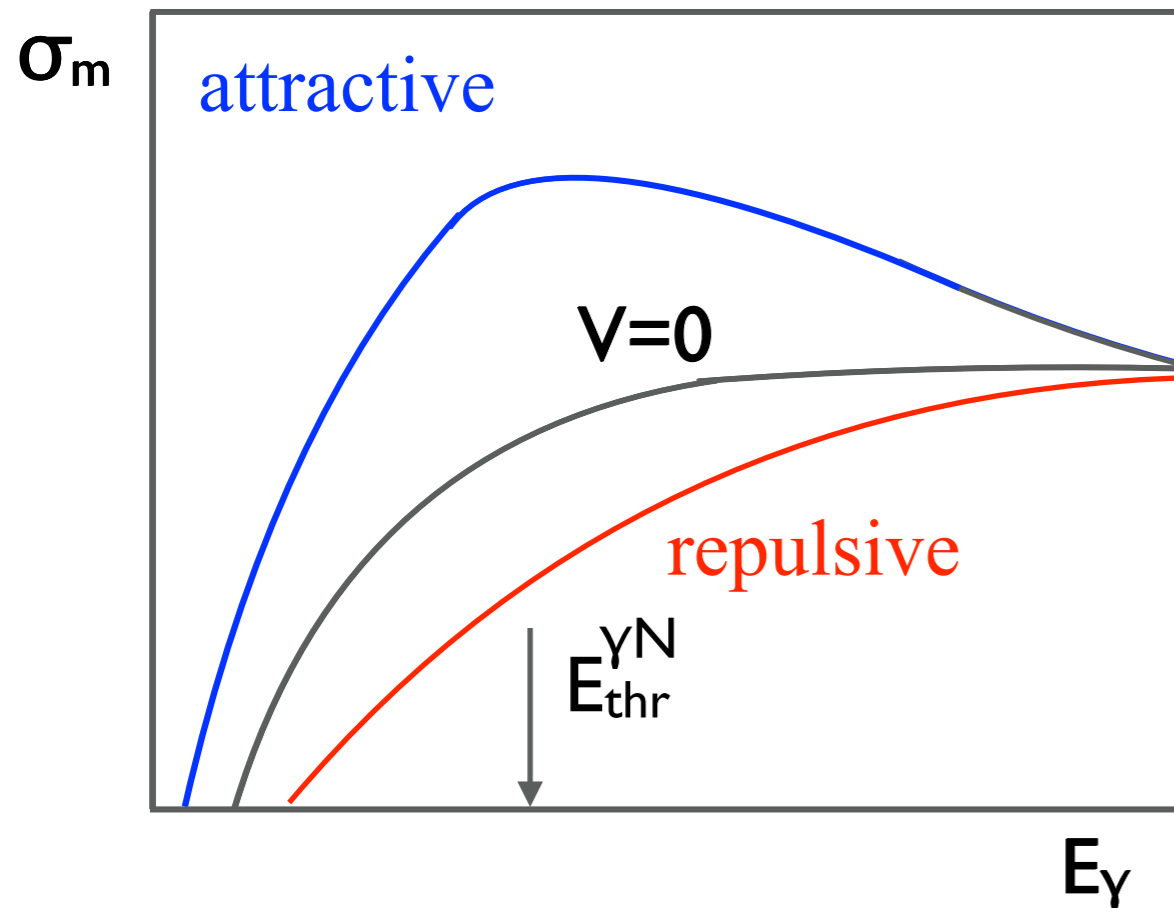
repulsive interaction  $\rightarrow$  mass increase  $\rightarrow$   
higher threshold  $\rightarrow$  smaller phase space  $\rightarrow$   
smaller cross section

repulsive interaction  $\rightarrow$  extra kick  $\rightarrow$   
shift to higher momenta

# Determining the real part of the meson-nucleus potential from excitation functions and momentum distributions

sensitive to nuclear density at the **production point**

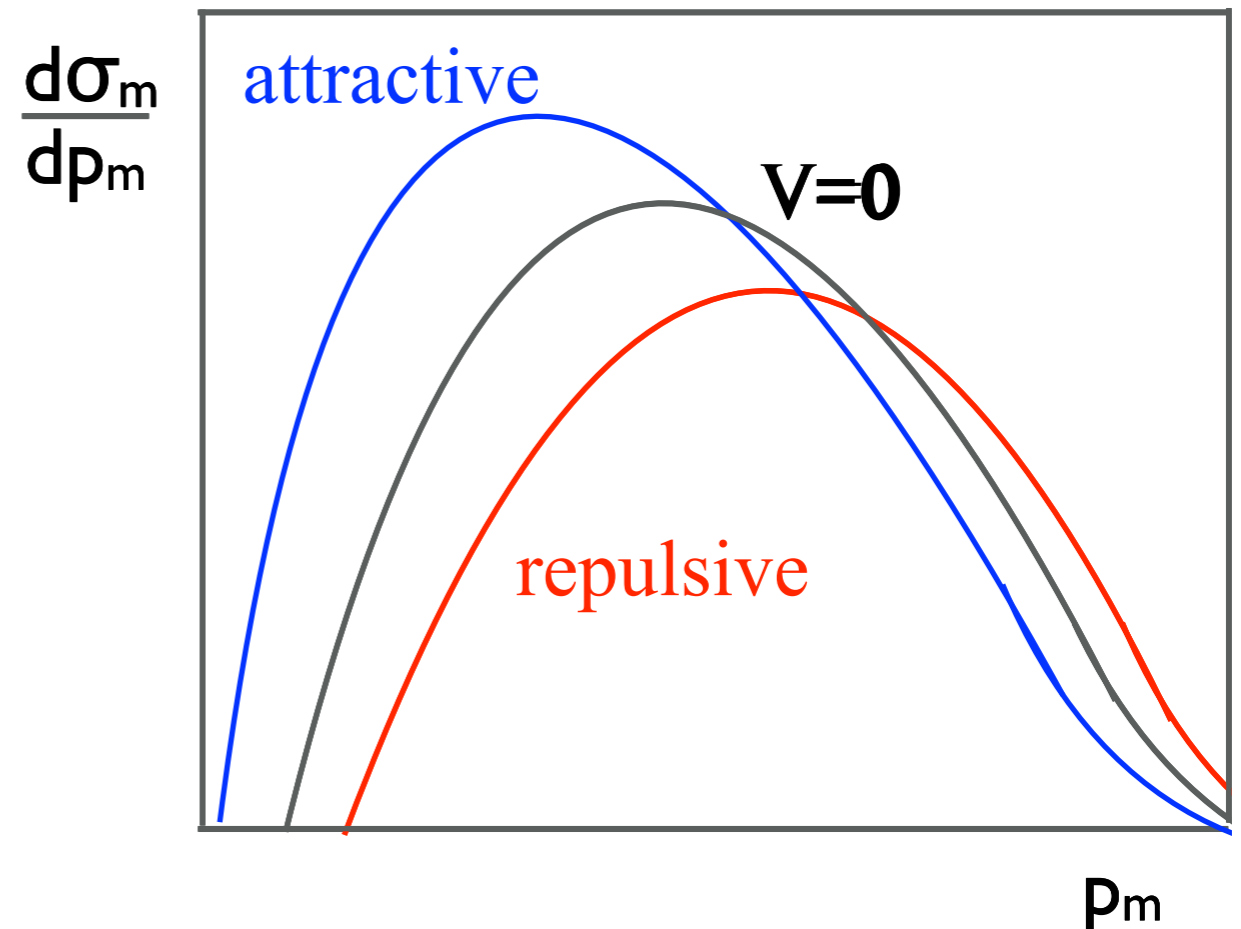
excitation function



attractive interaction  $\rightarrow$  mass drop  $\rightarrow$   
lower threshold  $\rightarrow$  larger phase space  $\rightarrow$   
larger cross section

repulsive interaction  $\rightarrow$  mass increase  $\rightarrow$   
higher threshold  $\rightarrow$  smaller phase space  $\rightarrow$   
smaller cross section

momentum distribution



repulsive interaction  $\rightarrow$  extra kick  $\rightarrow$   
shift to higher momenta

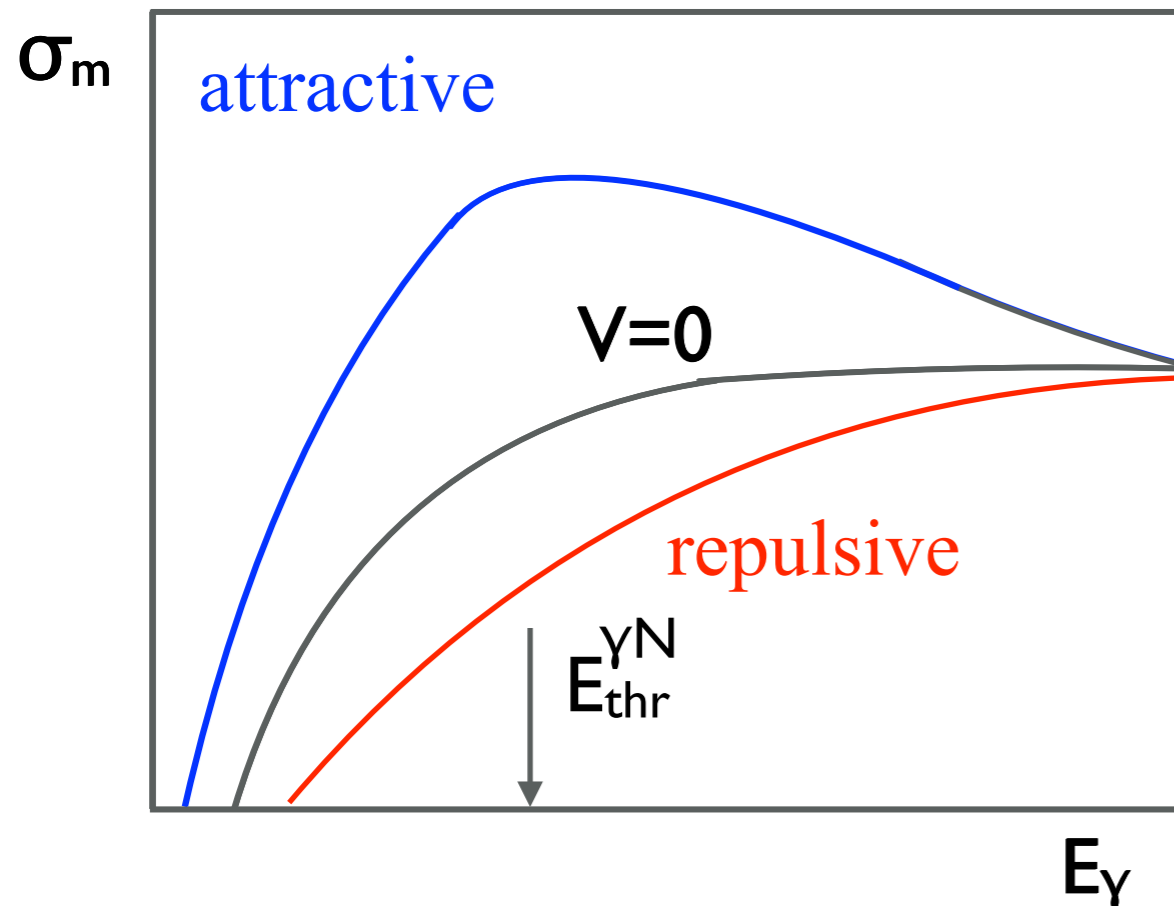
attractive interaction  $\rightarrow$   
meson slowed down  $\rightarrow$   
shift to lower momenta



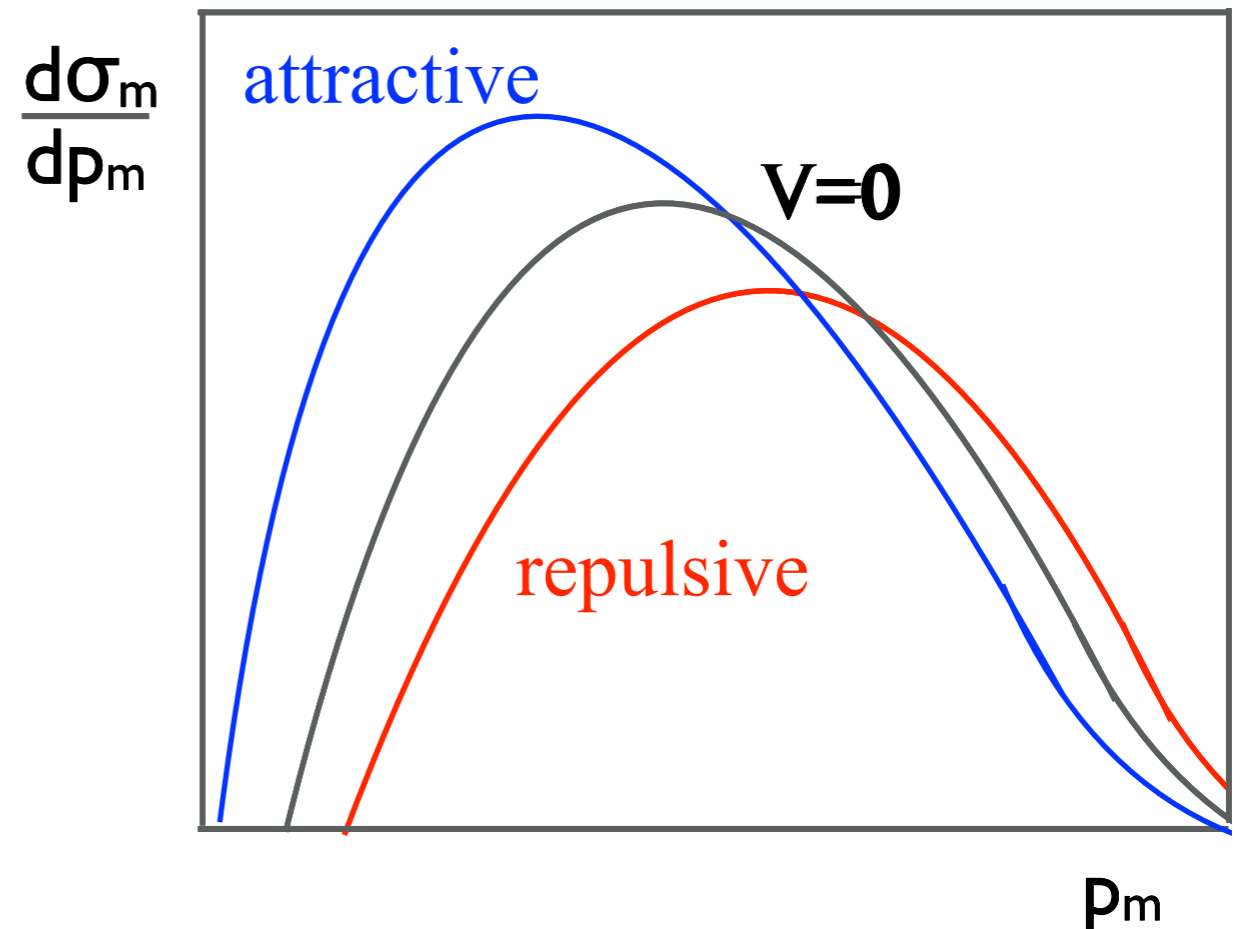
# Determining the real part of the meson-nucleus potential from excitation functions and momentum distributions

sensitive to nuclear density at the **production point**

excitation function



momentum distribution



attractive interaction  $\rightarrow$  mass drop  $\rightarrow$   
lower threshold  $\rightarrow$  larger phase space  $\rightarrow$   
larger cross section

repulsive interaction  $\rightarrow$  mass increase  $\rightarrow$   
higher threshold  $\rightarrow$  smaller phase space  $\rightarrow$   
smaller cross section

repulsive interaction  $\rightarrow$  extra kick  $\rightarrow$   
shift to higher momenta

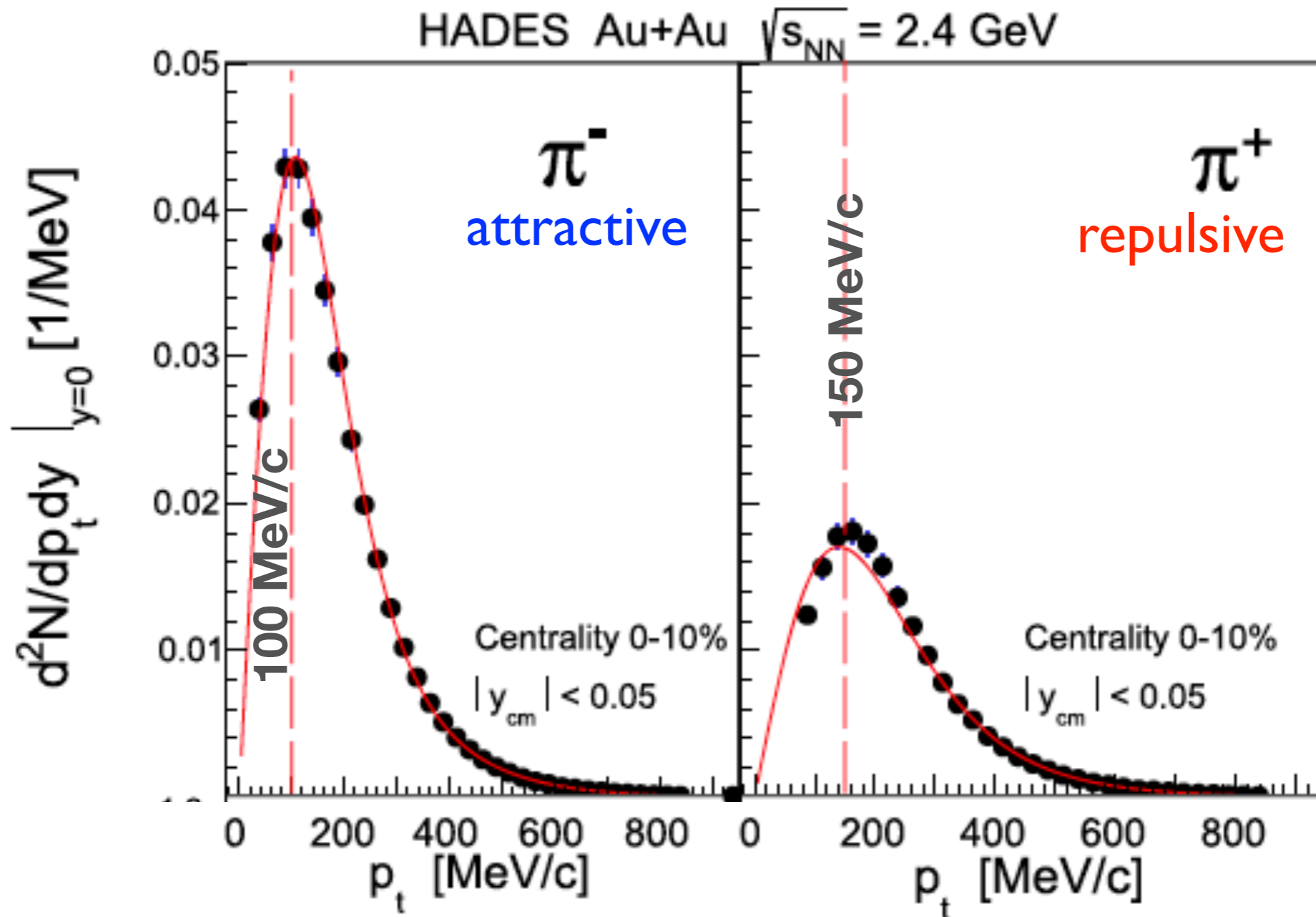
attractive interaction  $\rightarrow$   
meson slowed down  $\rightarrow$   
shift to lower momenta

quantitative analysis requires transport model or collision model calculations

# Test of method

Coulomb interaction among charged pions and the fireball in heavy-ion collisions

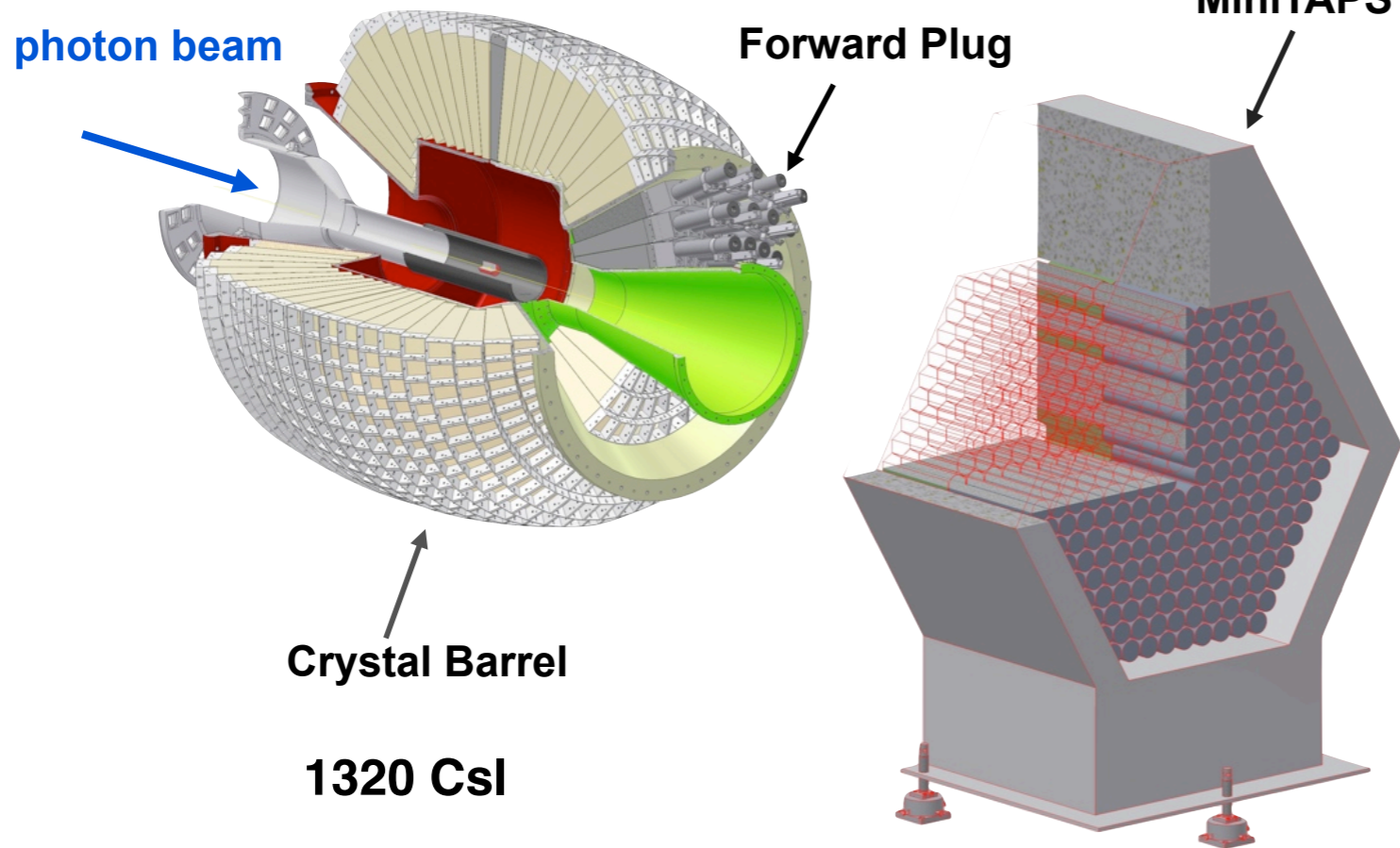
Eur. Phys. J. A 56 (2020) 259



spectrum shifted to smaller (larger) momenta for  $\pi^-$  ( $\pi^+$ ) mesons  
 $V_c = 13.6 \pm 0.6$  MeV; HADES Collaboration, Eur. Phys. J. A 48 (2022) 9

# CBELSA/TAPS Experiment

$E_\gamma = 1.2 - 2.9 \text{ GeV}$



Crystal Barrel

1320 CsI

11°-156°

216 BaF<sub>2</sub>  
MiniTAPS

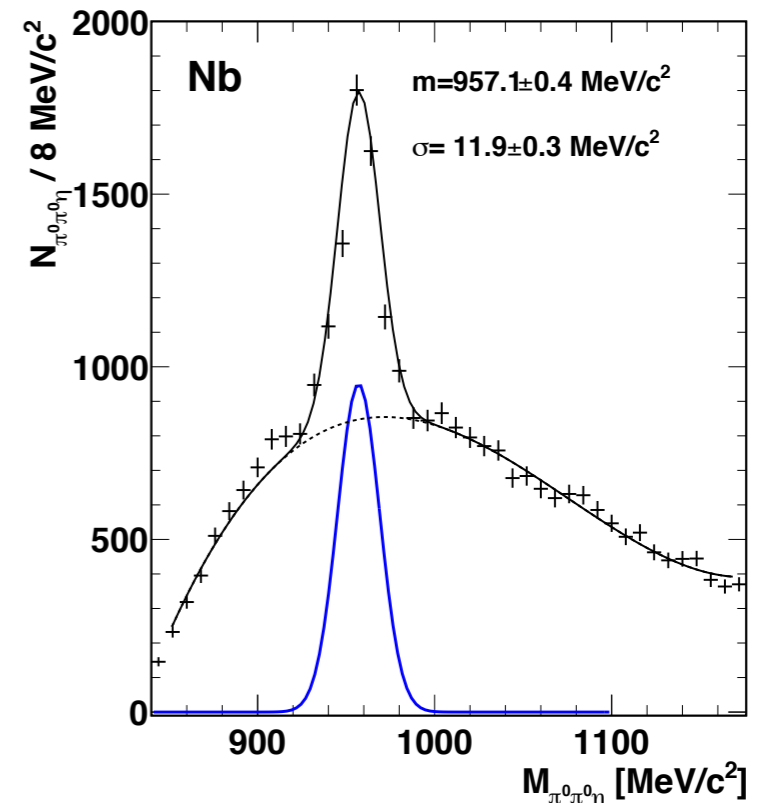
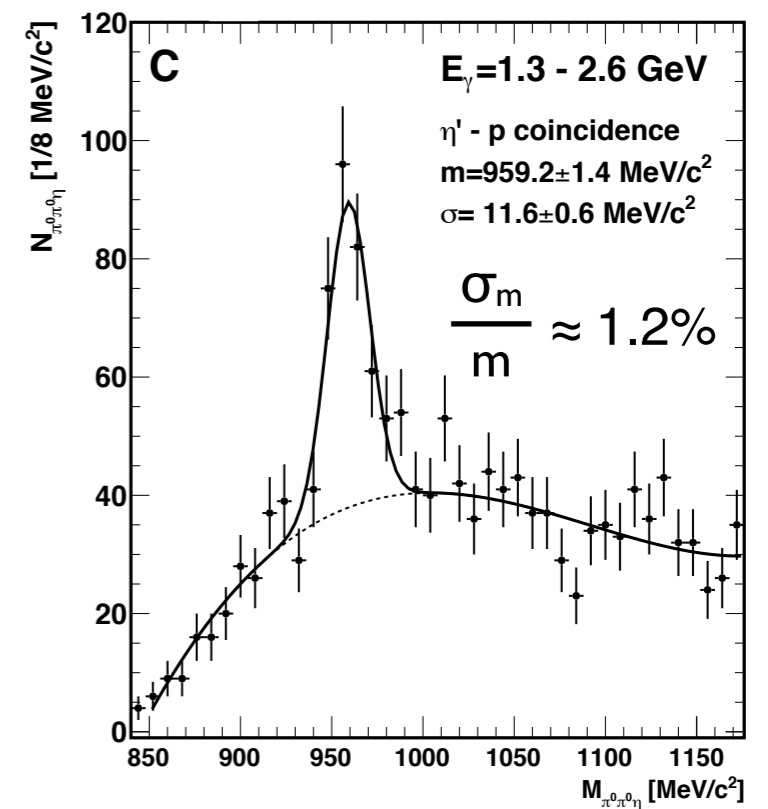
Forward Plug

1°-11°

targets: LH<sub>2</sub>, C, Ca, Nb, Pb

4π photon detector: ideally suited for identification of multi-photon final states

$\eta' \rightarrow \pi^0 \pi^0 \eta \rightarrow 6\gamma$  BR 8.5%



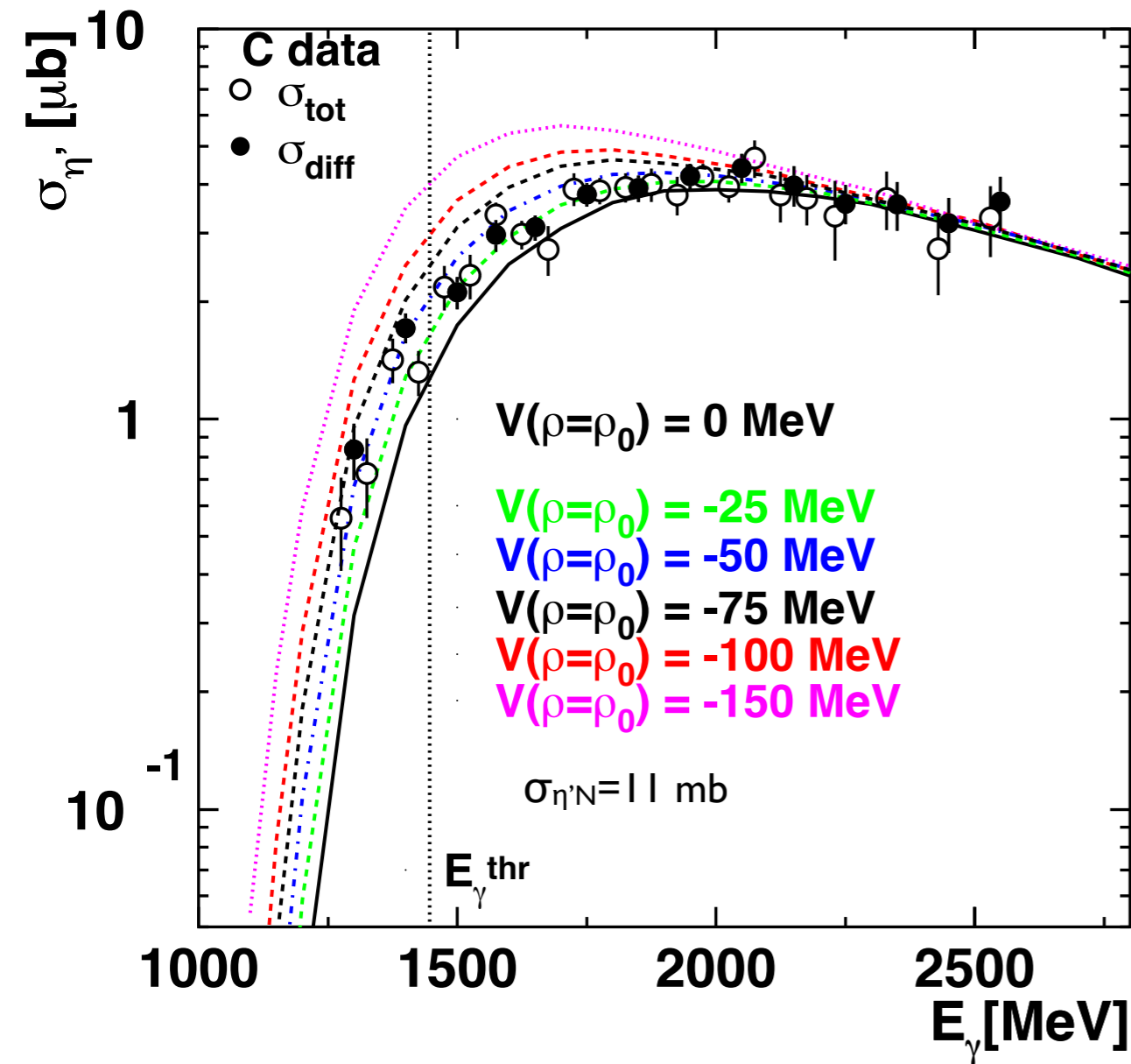
# Determining the real part of the $\eta'$ - nucleus potential from the excitation function

calc.: E. Paryev, J. Phys. G 40 (2013) 025201

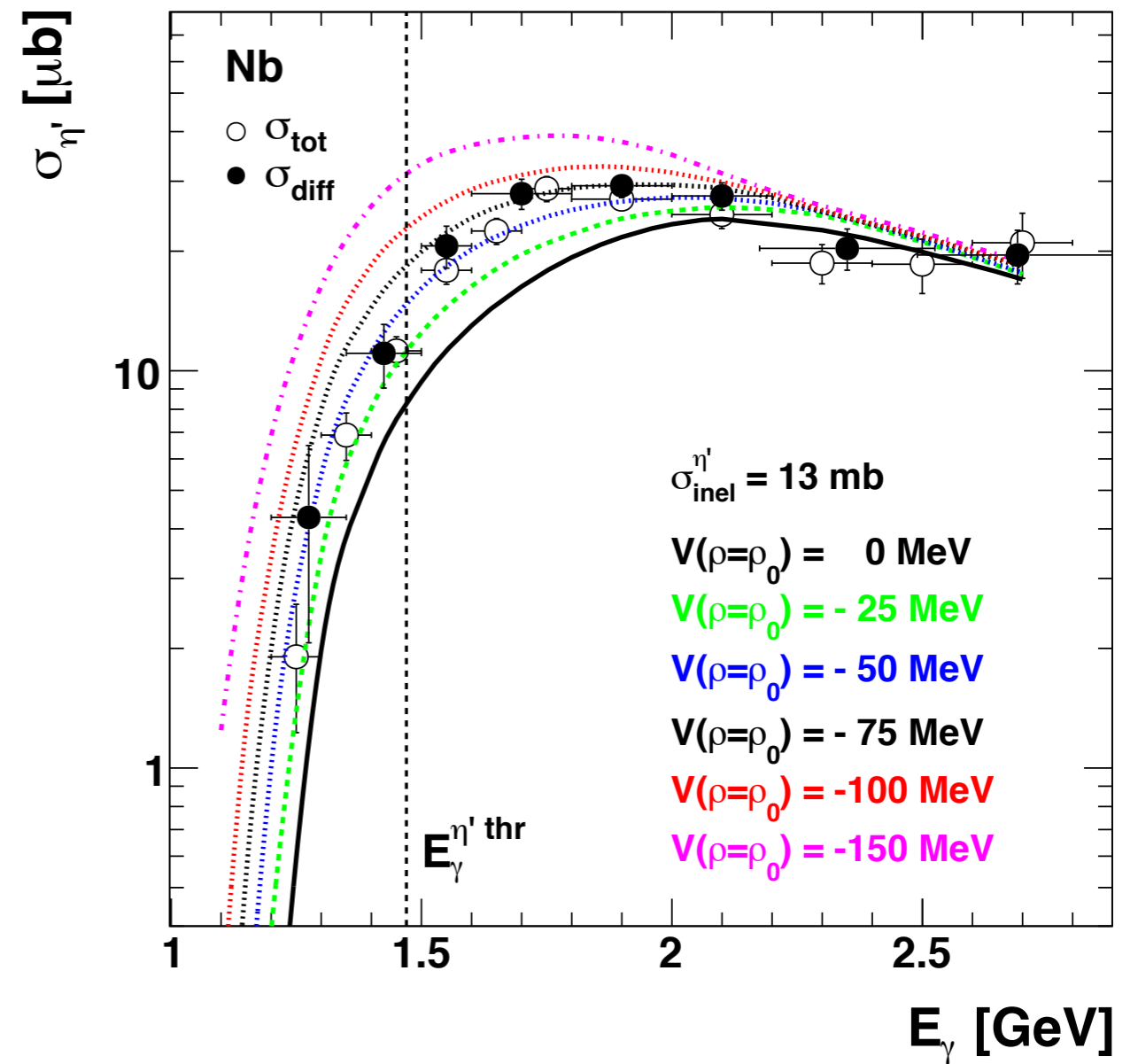
CBELSA/TAPS @ ELSA

M. Nanova et al., PLB 727 (2013) 417

M. Nanova et al., PRC 94 (2016) 025205



$$V_{\eta'}(\rho=\rho_0) = -(40 \pm 6) \text{ MeV}$$



$$V_{\eta'}(\rho=\rho_0) = -(40 \pm 12) \text{ MeV}$$

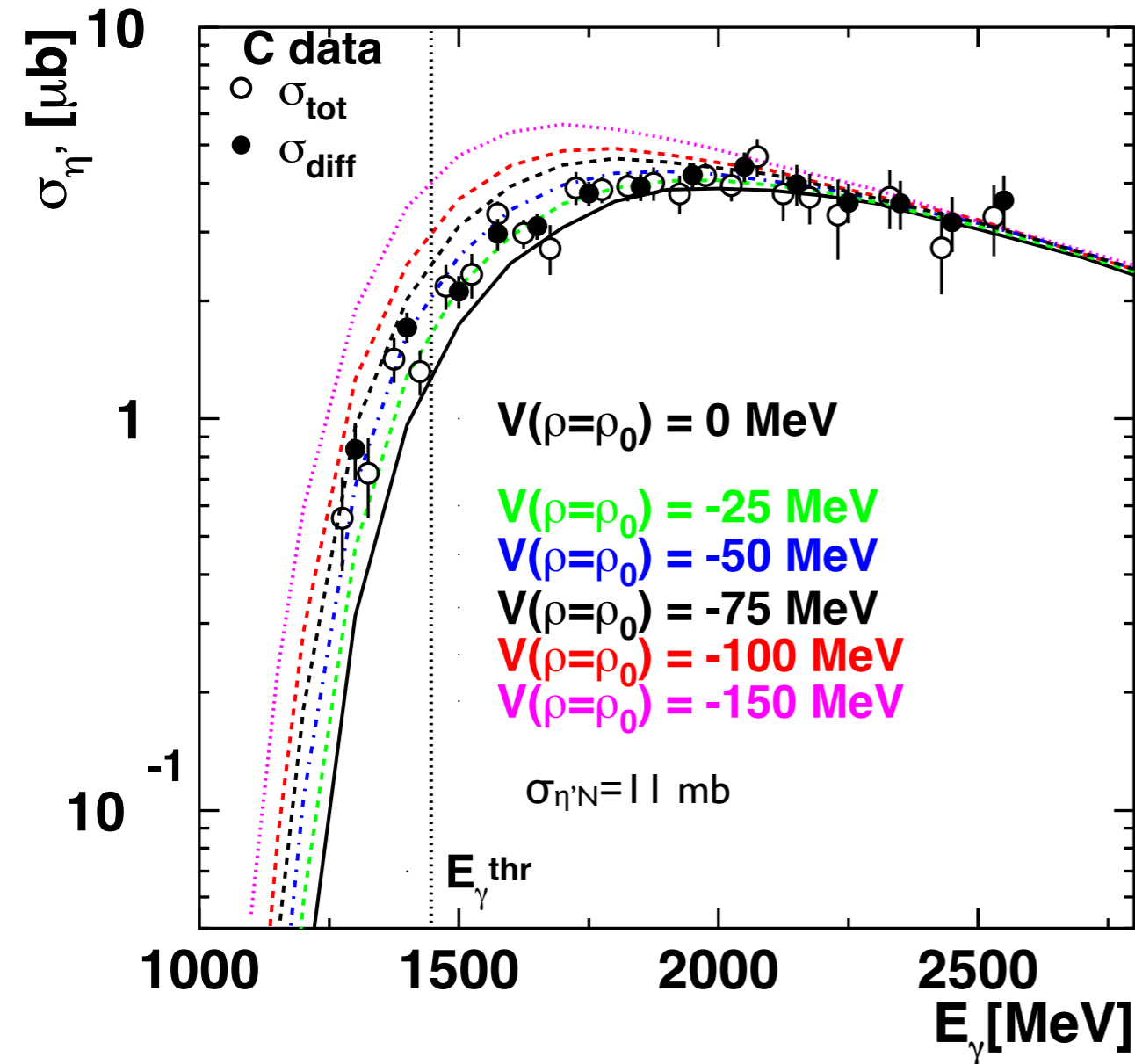
# Determining the real part of the $\eta'$ - nucleus potential from the excitation function

calc.: E. Paryev, J. Phys. G 40 (2013) 025201

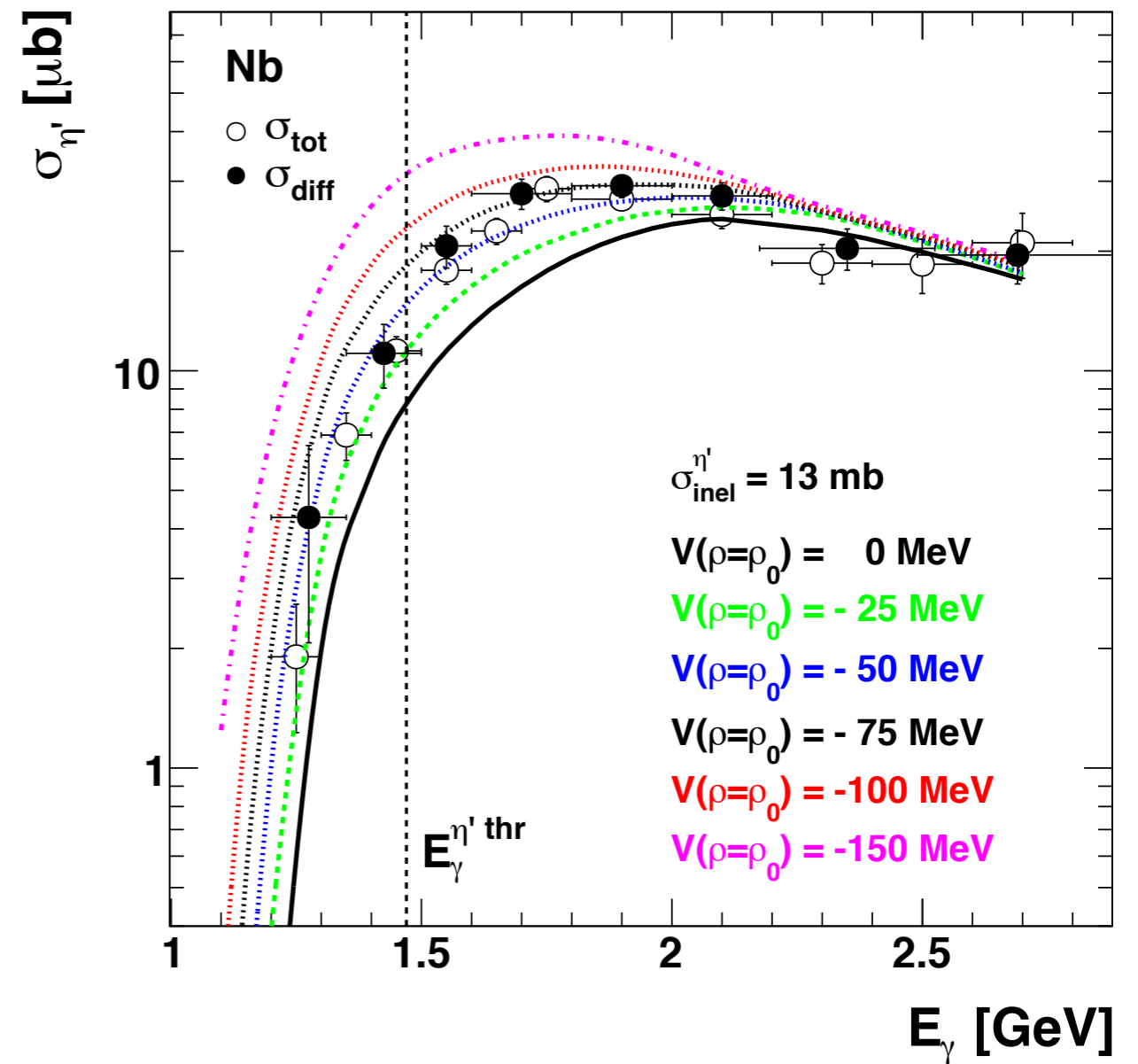
CBELSA/TAPS @ ELSA

M. Nanova et al., PLB 727 (2013) 417

M. Nanova et al., PRC 94 (2016) 025205



$$V_{\eta'}(\rho=\rho_0) = -(40 \pm 6) \text{ MeV}$$



$$V_{\eta'}(\rho=\rho_0) = -(40 \pm 12) \text{ MeV}$$

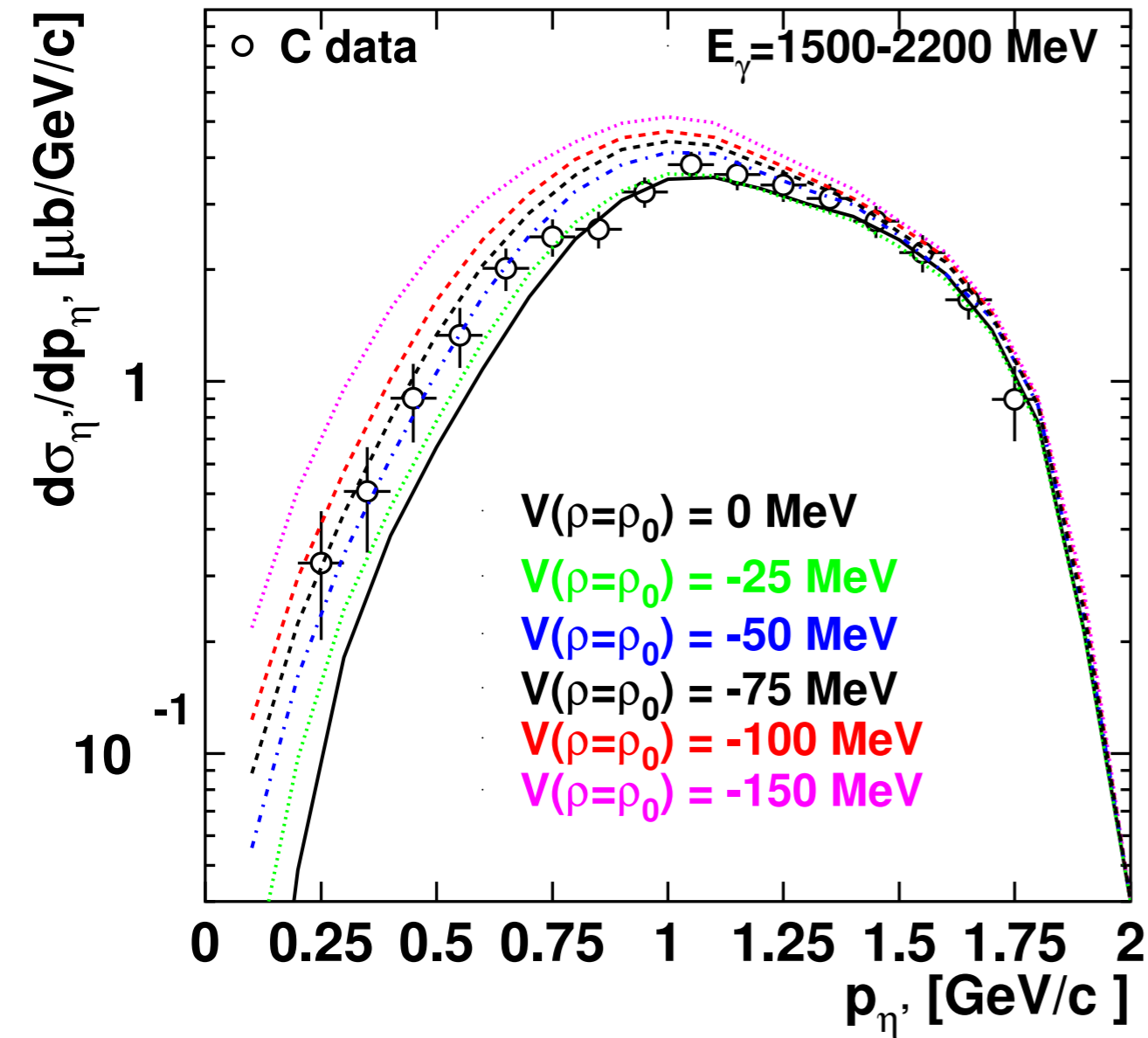
data disfavour strong mass shifts

# Determining the real part of the $\eta'$ - nucleus potential from the momentum distribution

CBELSA/TAPS @ ELSA

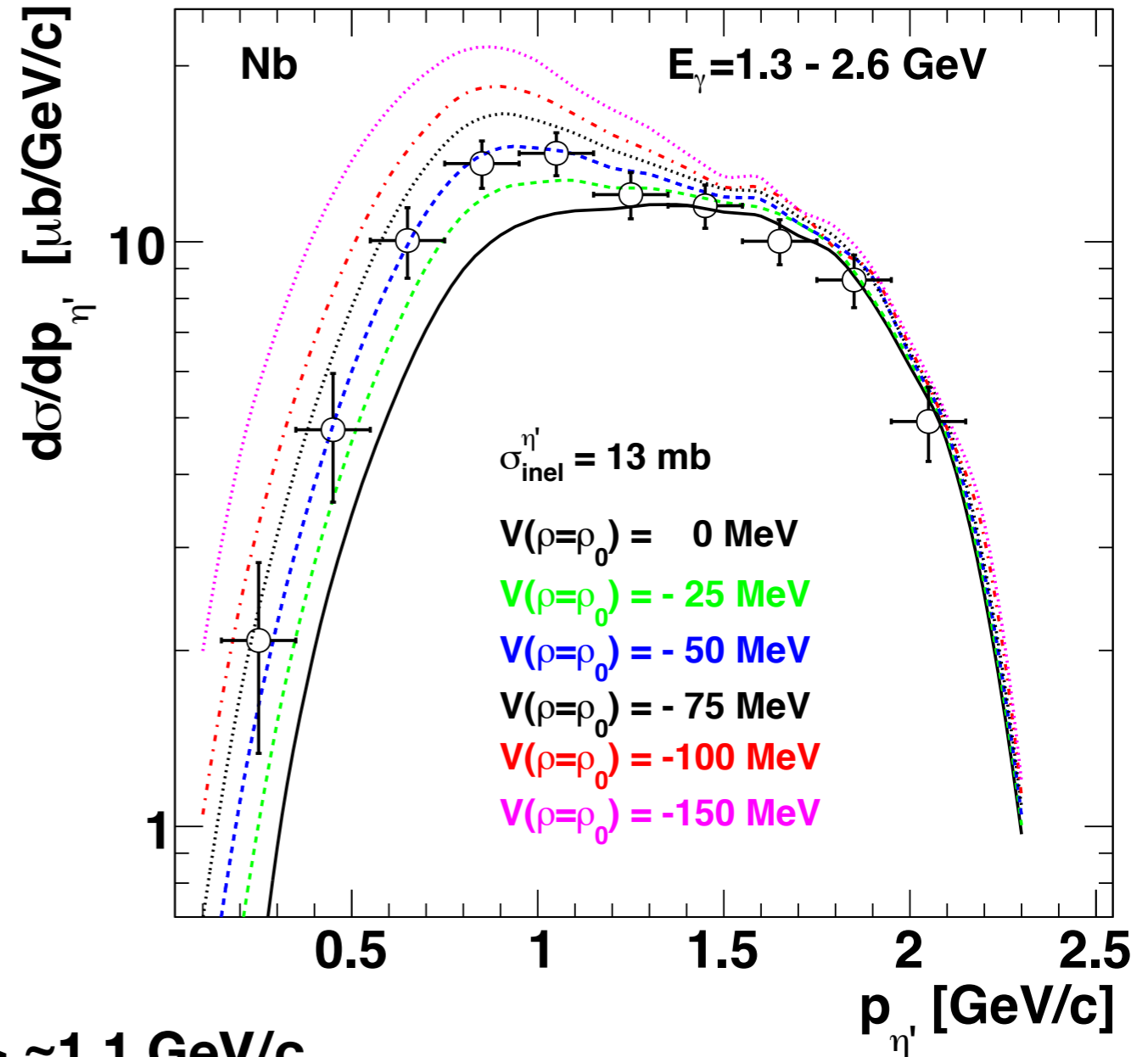
M. Nanova et al., PLB 727 (2013) 417

M. Nanova et al., PRC 94 (2016) 025205



$\langle p \rangle \approx 1.1$  GeV/c

$$V_{\eta'}(\rho=\rho_0) = -(32 \pm 11) \text{ MeV}$$



$$V_{\eta'}(\rho=\rho_0) = -(45 \pm 20) \text{ MeV}$$

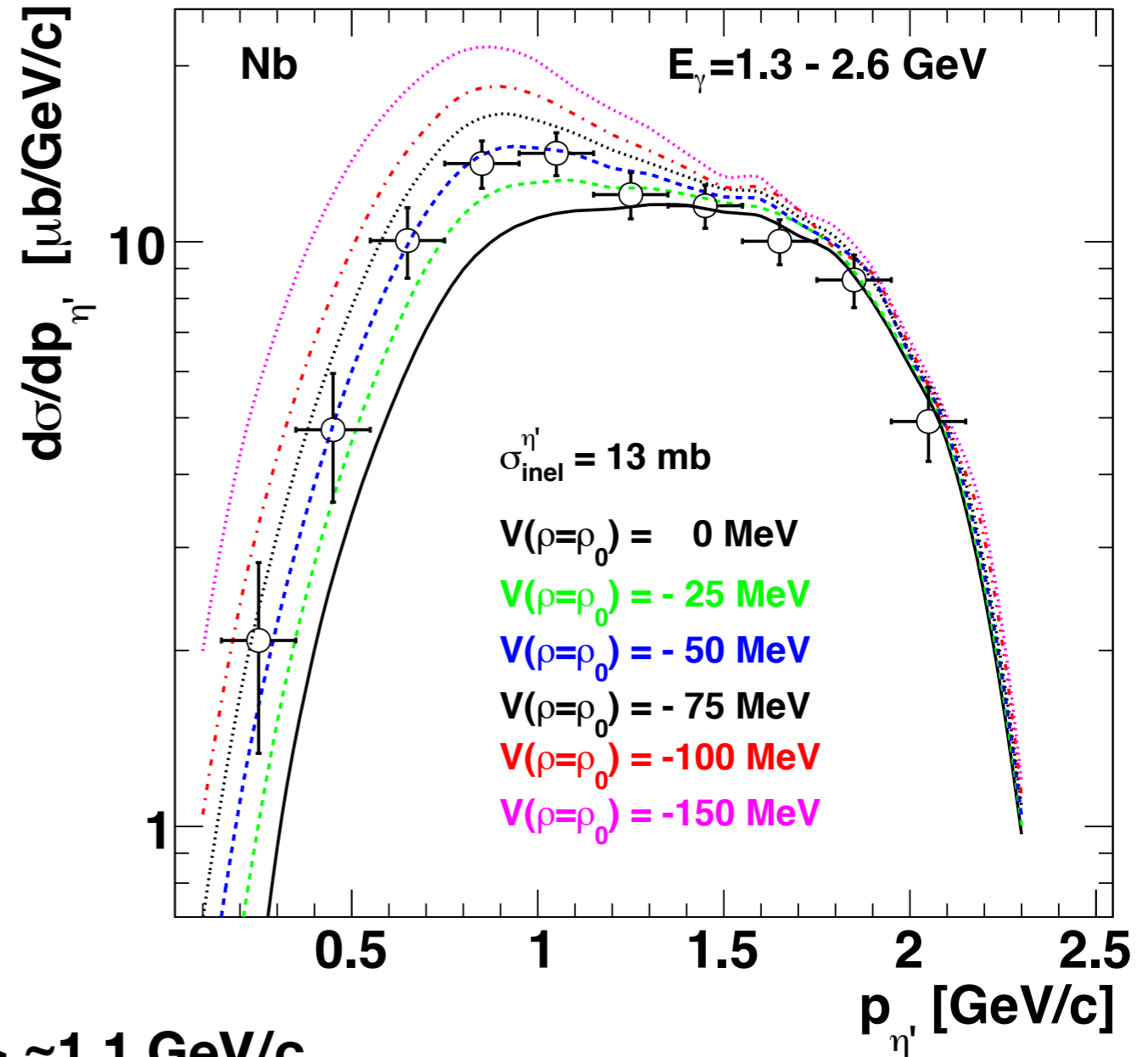
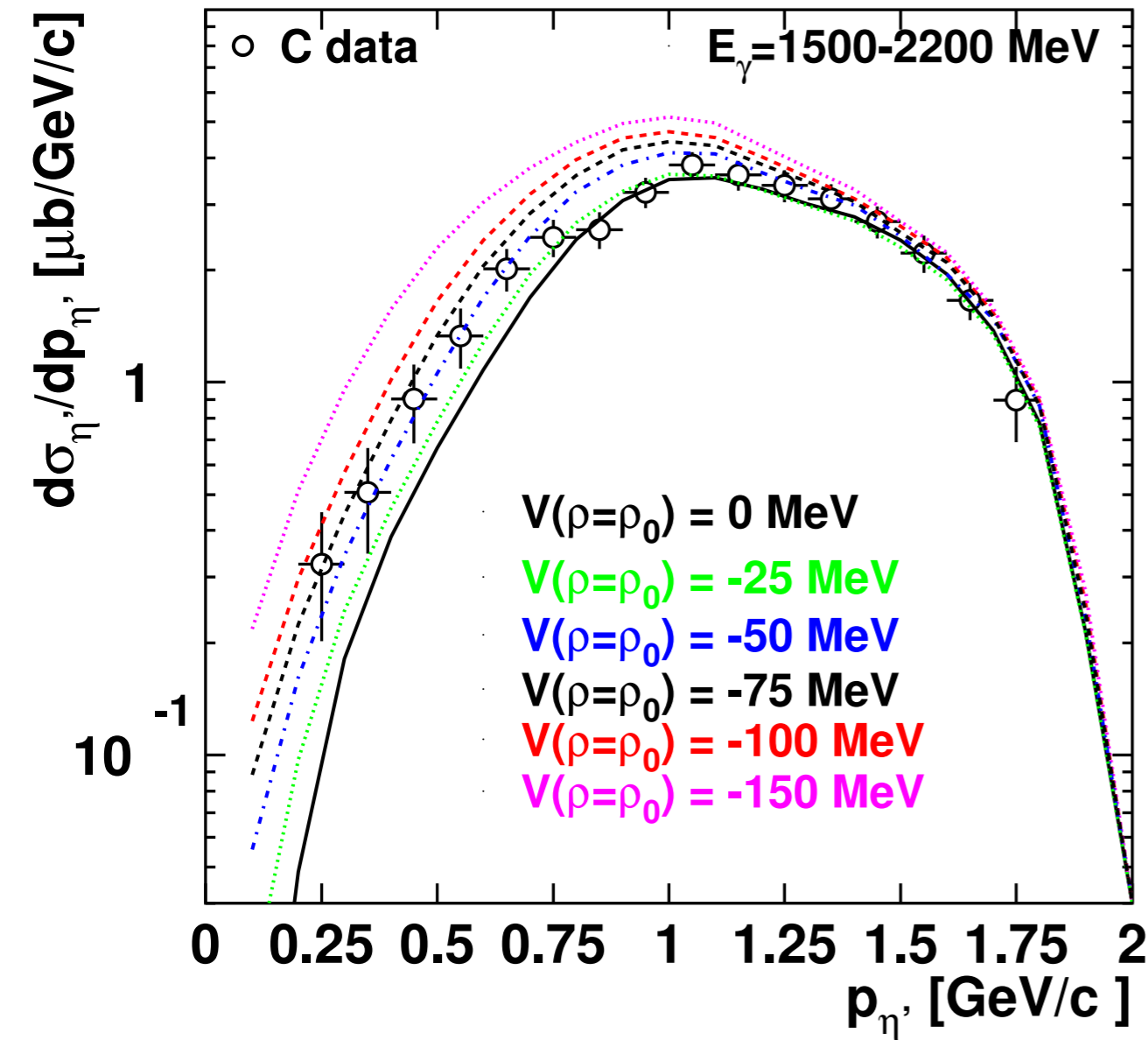


# Determining the real part of the $\eta'$ - nucleus potential from the momentum distribution

CBELSA/TAPS @ ELSA

M. Nanova et al., PLB 727 (2013) 417

M. Nanova et al., PRC 94 (2016) 025205



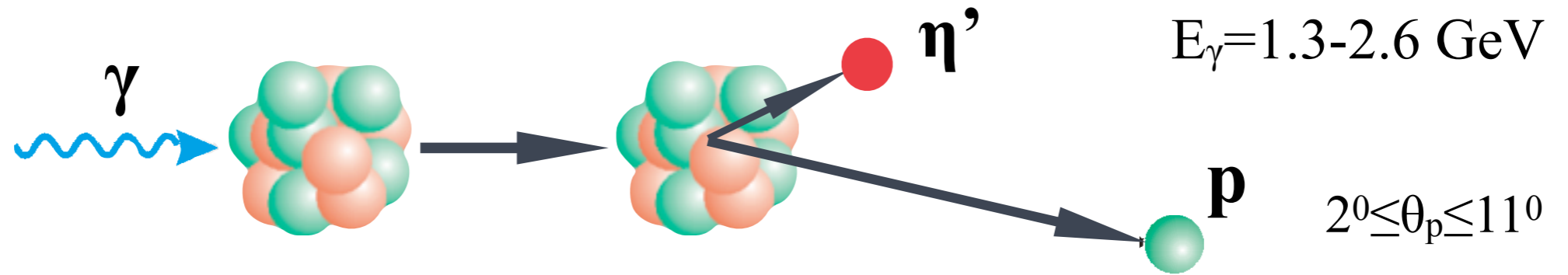
$\langle p \rangle \approx 1.1$  GeV/c

$$V_{\eta'}(\rho=\rho_0) = -(32 \pm 11) \text{ MeV}$$

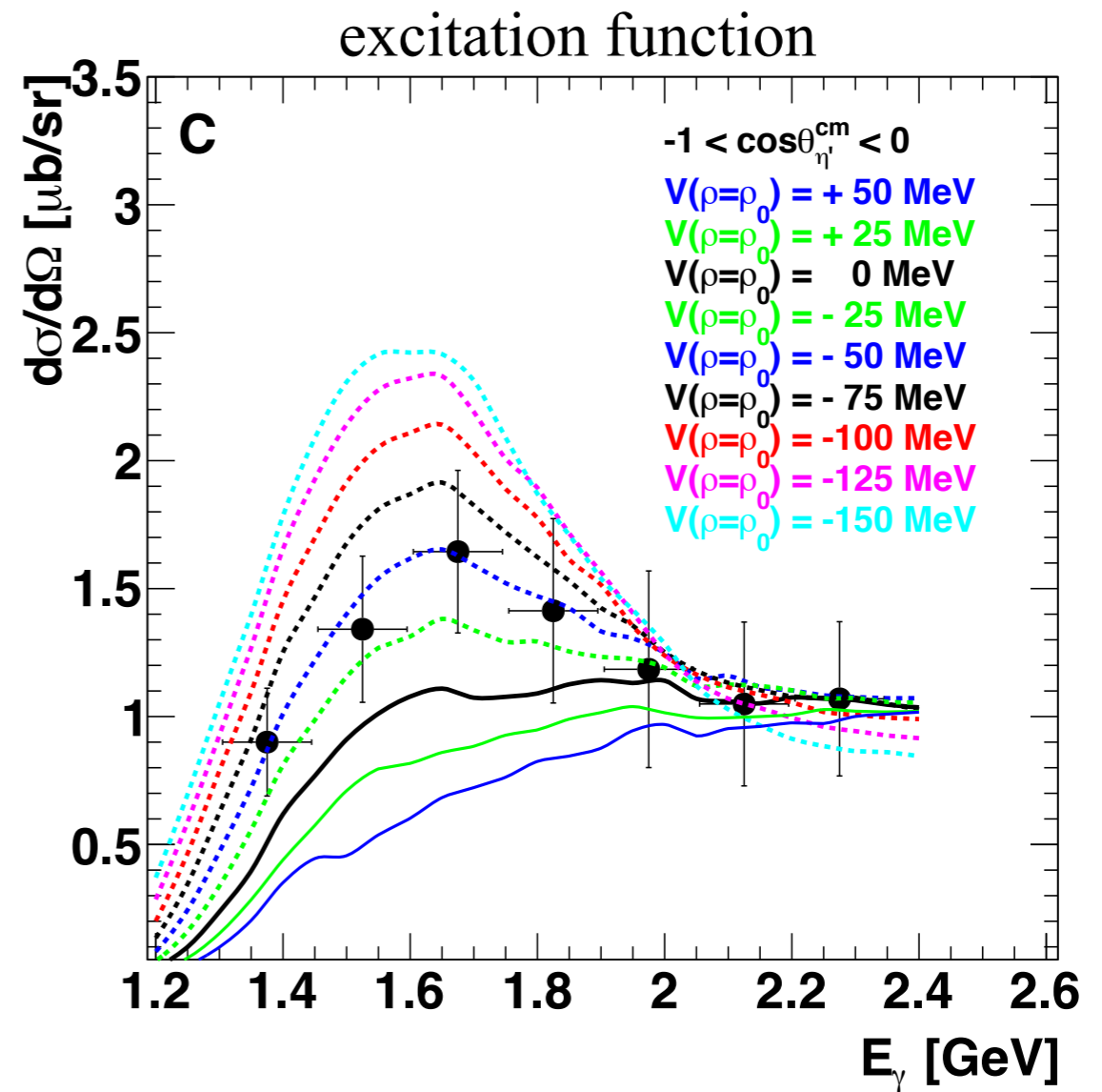
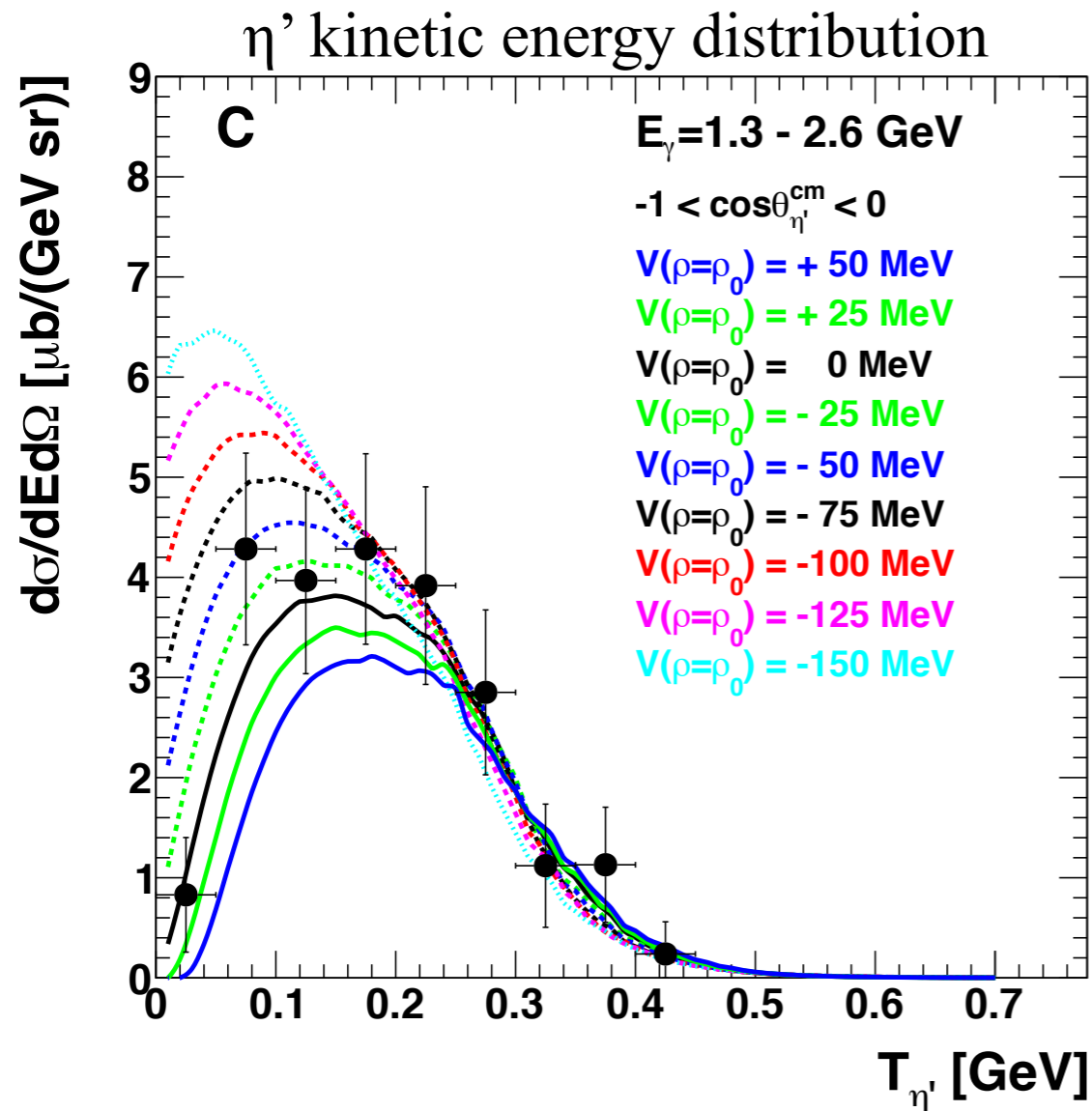
$$V_{\eta'}(\rho=\rho_0) = -(45 \pm 20) \text{ MeV}$$

data disfavour strong mass shifts

# Real part of the $\eta'$ -nucleus potential at low momenta

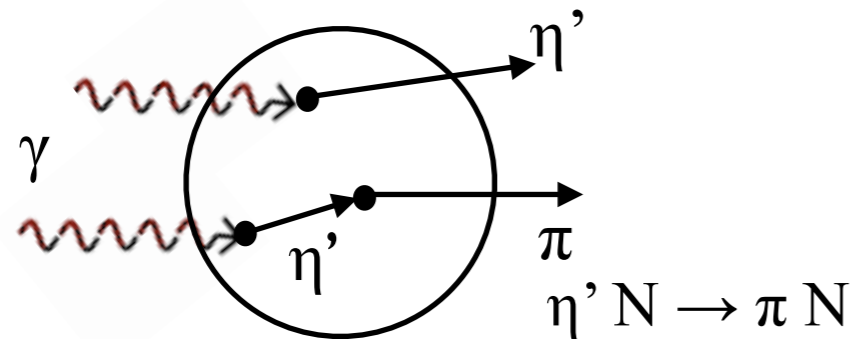


M. Nanova et al., EPJ A 54 (2018) 182



best fit for  $V(\rho=\rho_0) = -[44 \pm 16(\text{stat}) \pm 15(\text{syst})] \text{ MeV}$

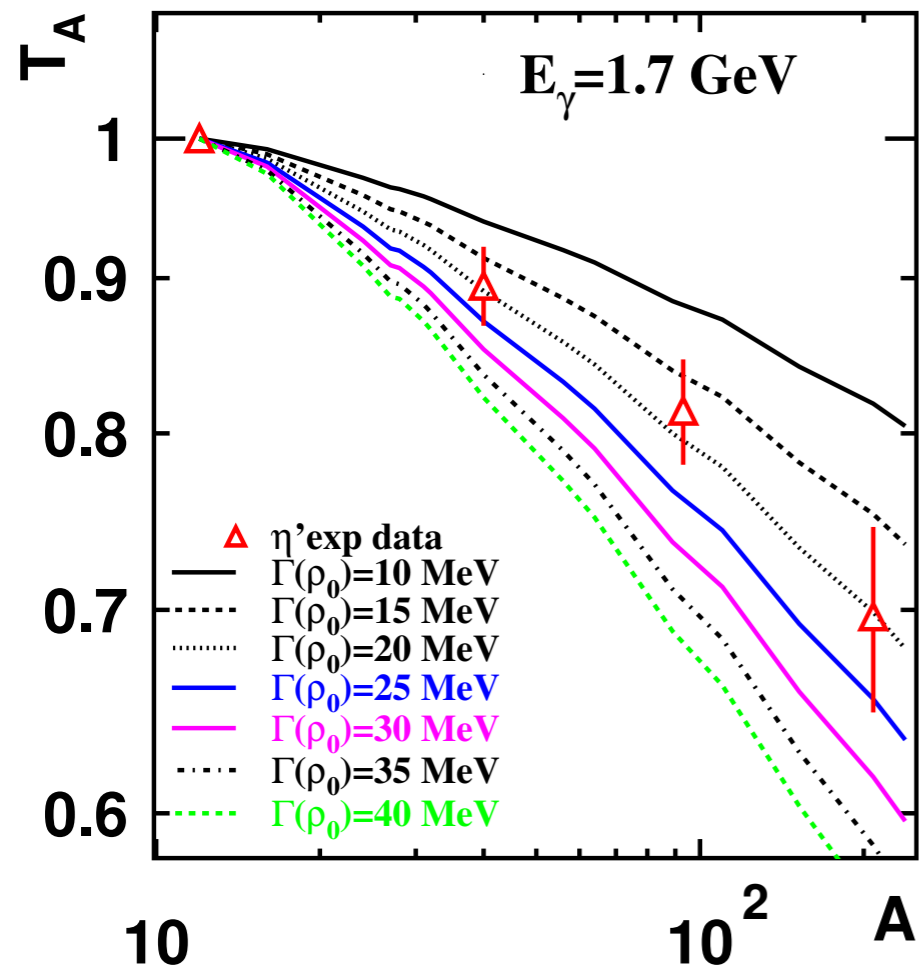
# Determining the imaginary part of the $\eta'$ - nucleus potential from transparency ratio measurements



$$T_A = \frac{\sigma_{\gamma A \rightarrow \eta' X}}{A \cdot \sigma_{\gamma N \rightarrow \eta' X}}$$

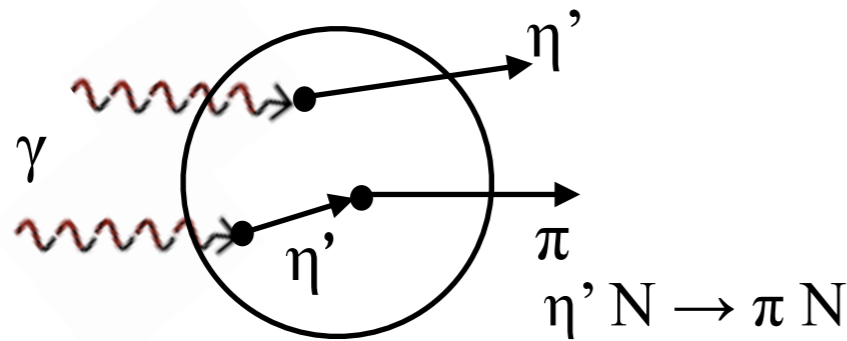
mass dependence of  $T_A$

M. Nanova et al., PLB 710 (2012) 600



$\Gamma_{\eta'}(\rho=\rho_0) = 15-25 \text{ MeV}$

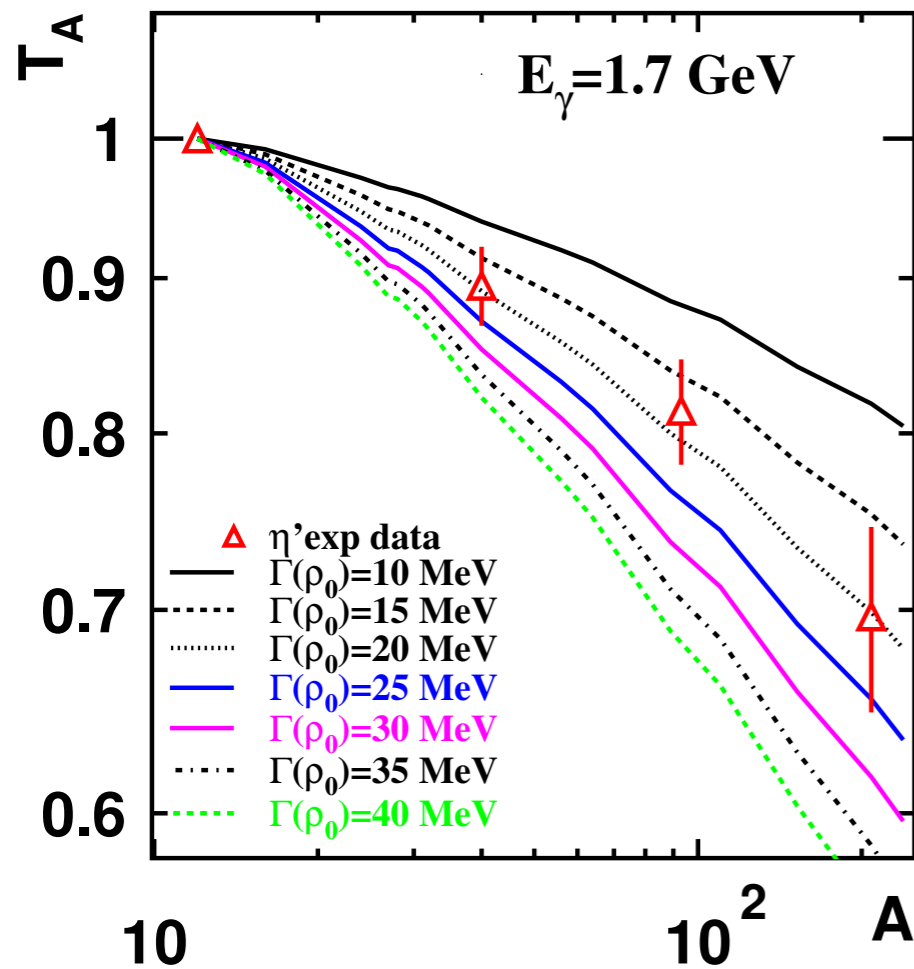
# Determining the imaginary part of the $\eta'$ - nucleus potential from transparency ratio measurements



$$T_A = \frac{\sigma_{\gamma A \rightarrow \eta' X}}{A \cdot \sigma_{\gamma N \rightarrow \eta' X}}$$

mass dependence of  $T_A$

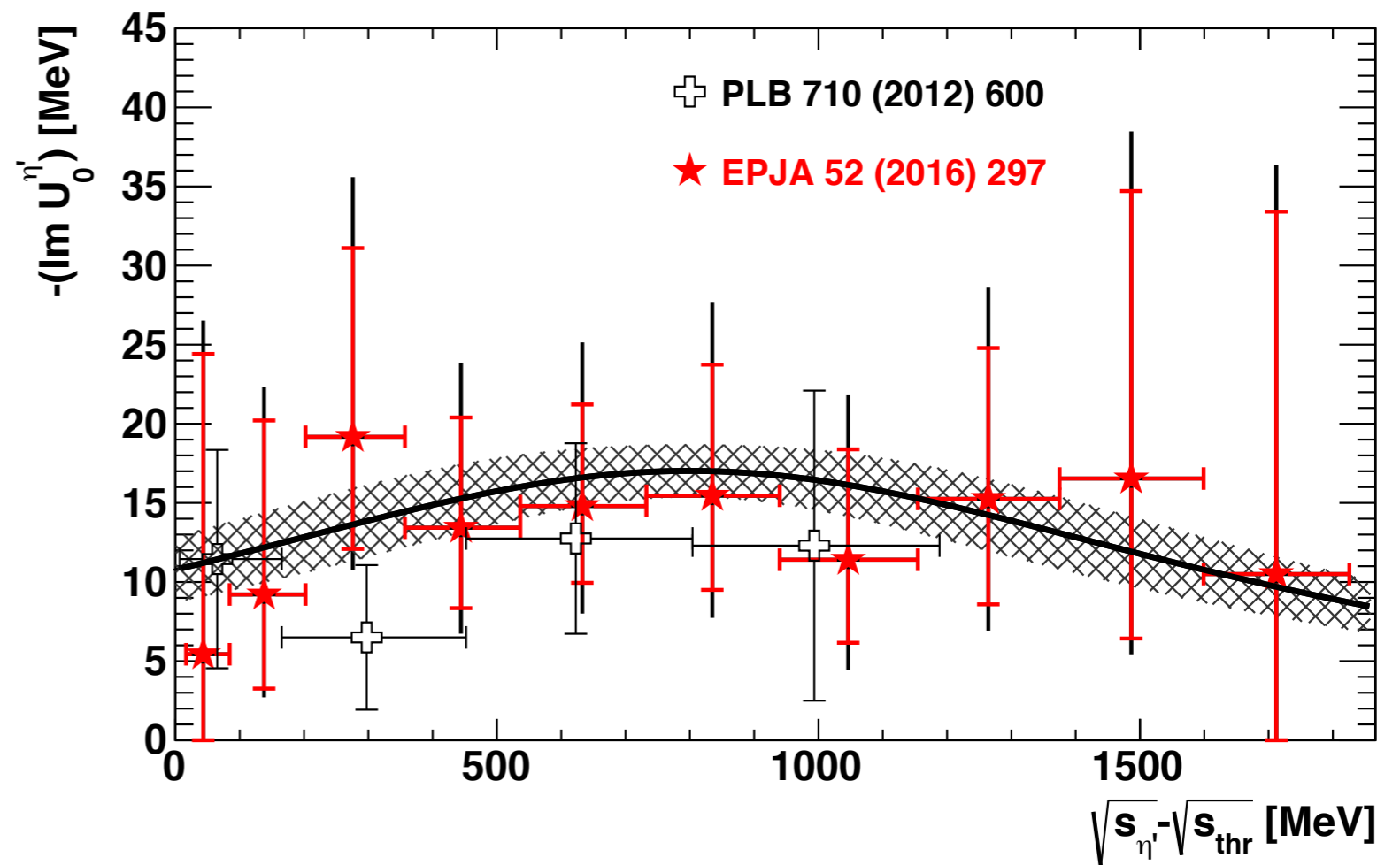
M. Nanova et al., PLB 710 (2012) 600



$\Gamma_{\eta'}(\rho = \rho_0) = 15\text{-}25 \text{ MeV}$

momentum dependence of  $W_0$

S. Friedrich et al., EPJA 52 (2016) 297

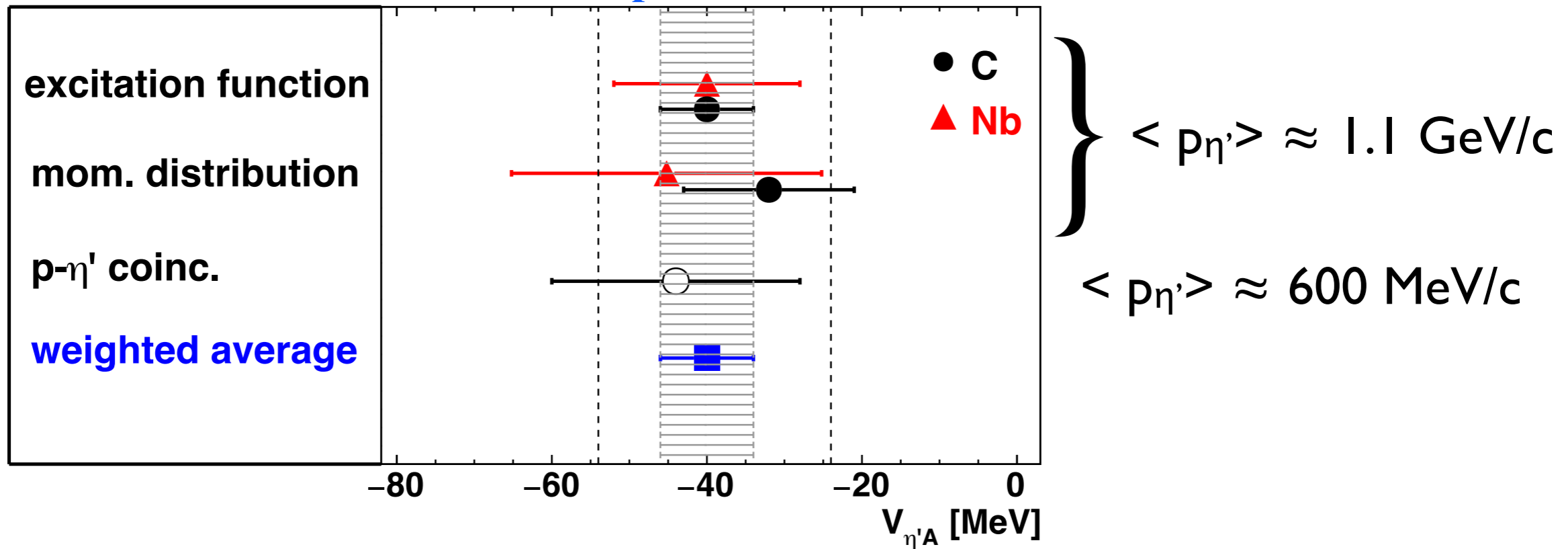


$W(\rho = \rho_0, p_{\eta'} = 0) = -[13 \pm 3(\text{stat}) \pm 3(\text{syst})] \text{ MeV}$

# Real and imaginary part of the $\eta'$ - nucleus potential

**real part:** M. Nanova et al., PRC 94 (2016) 025205  
 M. Nanova et al., EPJ A 54 (2018) 182  
 V. Metag, M. N. , E. Paryev , PPNP 97 (2017) 199

**model dependend!**



weighted average:  $V_0 = \Delta m(\rho = \rho_0) = -[39 \pm 7(\text{stat}) \pm 15(\text{syst})] \text{ MeV}$

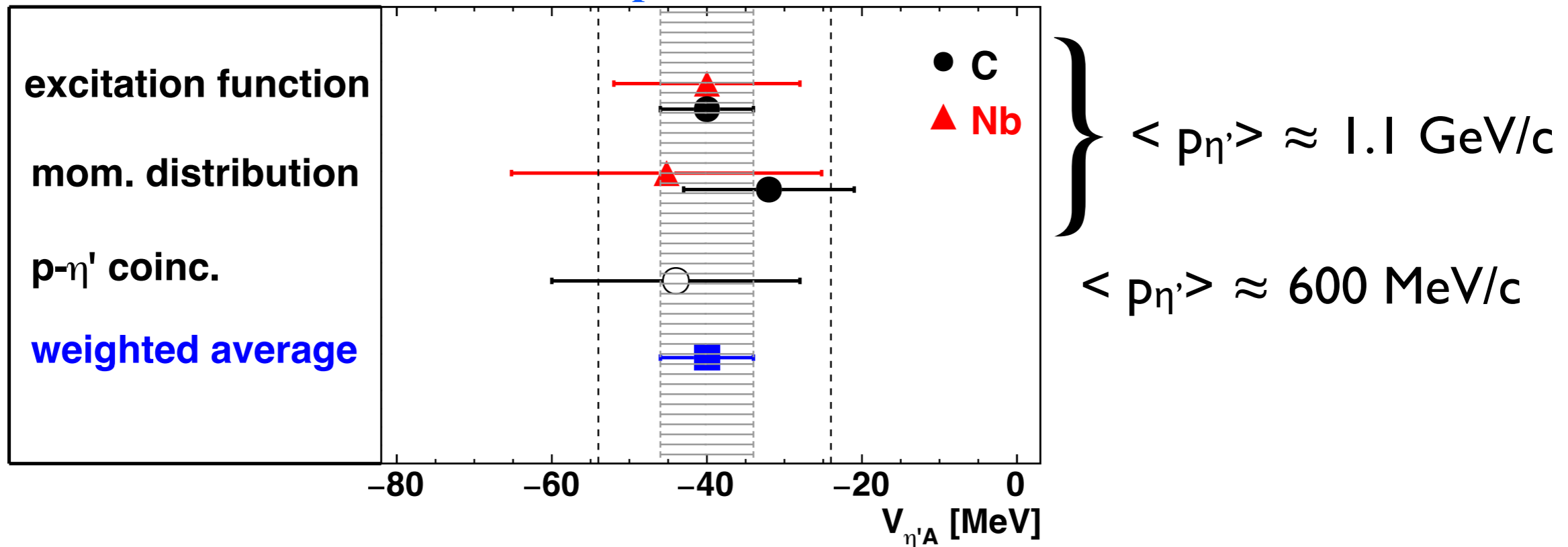
observed mass shift in agreement with QMC model predictions

S. Bass and T. Thomas, PLB 634 (2006) 368

# Real and imaginary part of the $\eta'$ - nucleus potential

**real part:** M. Nanova et al., PRC 94 (2016) 025205  
 M. Nanova et al., EPJ A 54 (2018) 182  
 V. Metag, M. N. , E. Paryev , PPNP 97 (2017) 199

**model dependend!**



weighted average:  $V_0 = \Delta m(\rho = \rho_0) = -[39 \pm 7(\text{stat}) \pm 15(\text{syst})] \text{ MeV}$

observed mass shift in agreement with QMC model predictions

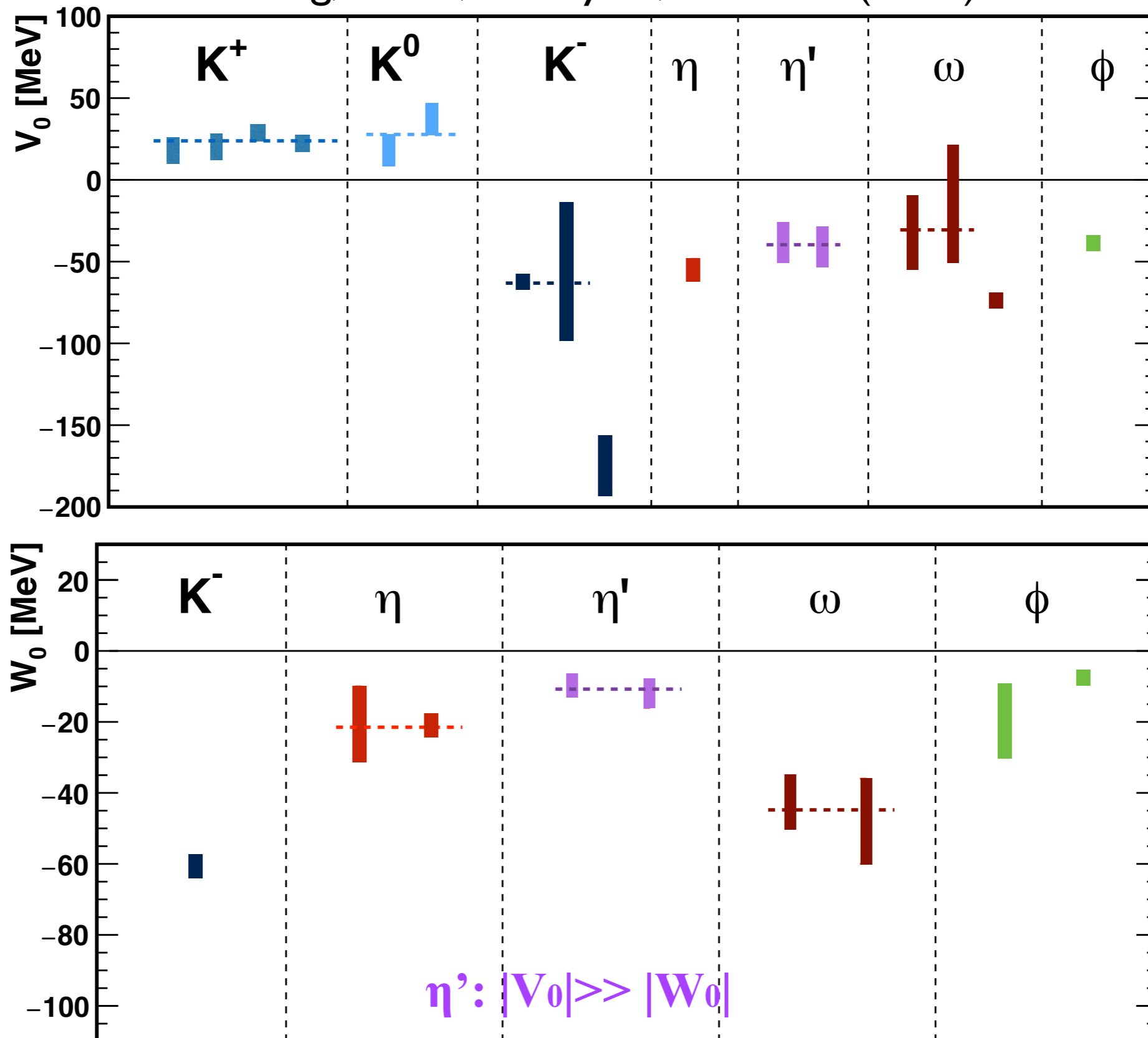
S. Bass and T. Thomas, PLB 634 (2006) 368

**imaginary part:** M. Nanova et al., PLB 727 (2013) 417  
 S. Friedrich et al., EPJA 52 (2016) 297

$$W_0 = \text{Im } U(\rho = \rho_0, p_{\eta'} \approx 0) = - [13 \pm 3(\text{stat}) \pm 3(\text{syst})] \text{ MeV}$$

# The meson-nucleus potential $U(\rho_0)=V(\rho_0)+iW(\rho_0)$

V. Metag, M. N. , E. Paryev , PPNP 97 (2017) 199



$\eta'$  promising candidate for mesic state:  $|W_0| \approx 13 \text{ MeV} \ll |V_0| \approx 40 \text{ MeV}$

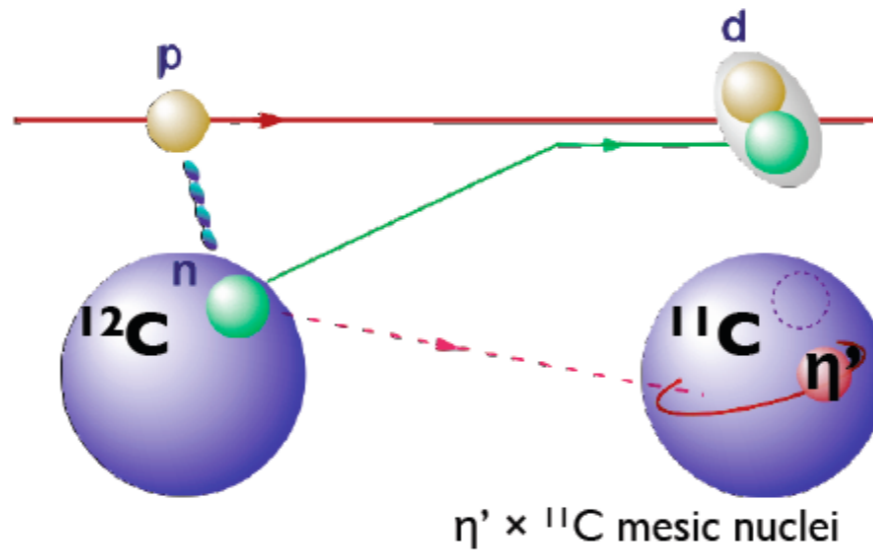
# Search for $\eta'$ - nucleus bound states I

recoilless production in  $^{12}\text{C}(p,d)$  reaction

**PRIME**

collaboration (2012)

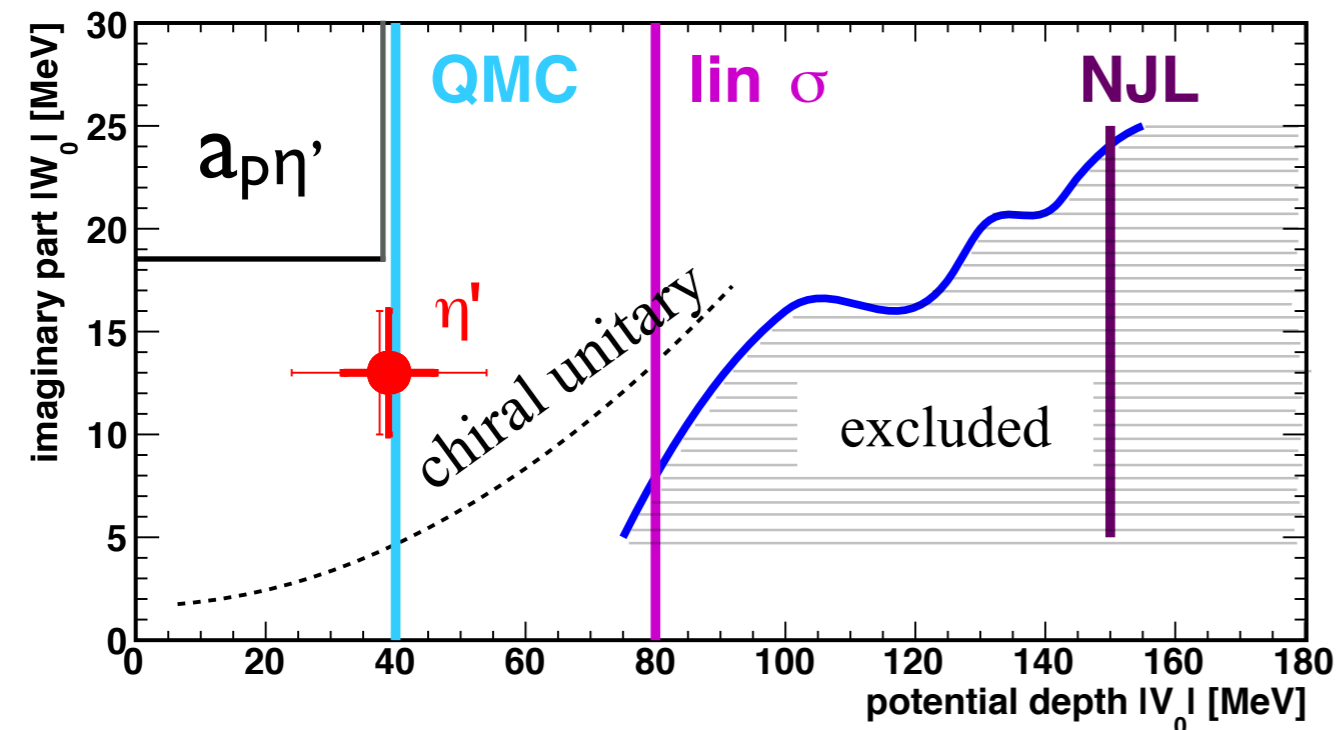
K. Itahashi et al., Exp. S 437



FRS@GSI

Y.K. Tanaka et al., PRL 117 (2016) 202501

Y.K. Tanaka et al., PRC 97 (2018) 015202





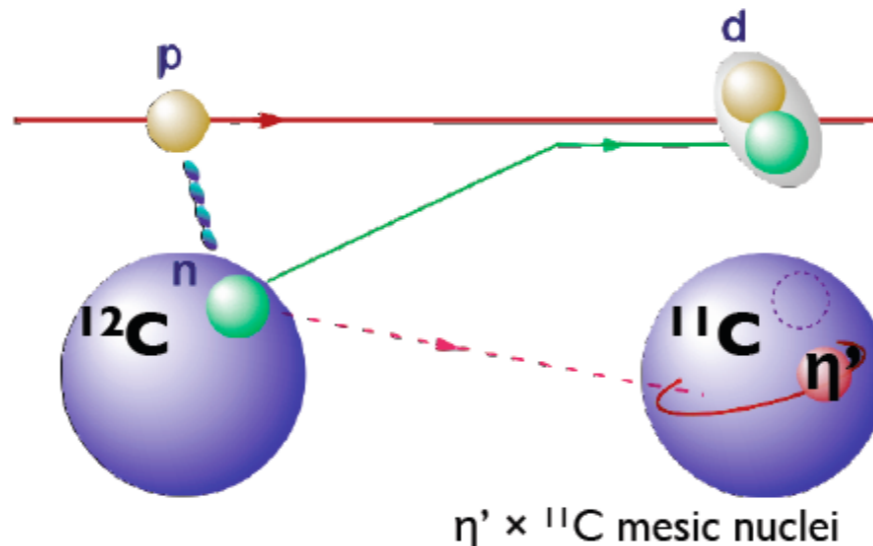
# Search for $\eta'$ - nucleus bound states I

recoilless production in  $^{12}\text{C}(p,d)$  reaction

**PRIME**

collaboration (2012)

K. Itahashi et al., Exp. S 437



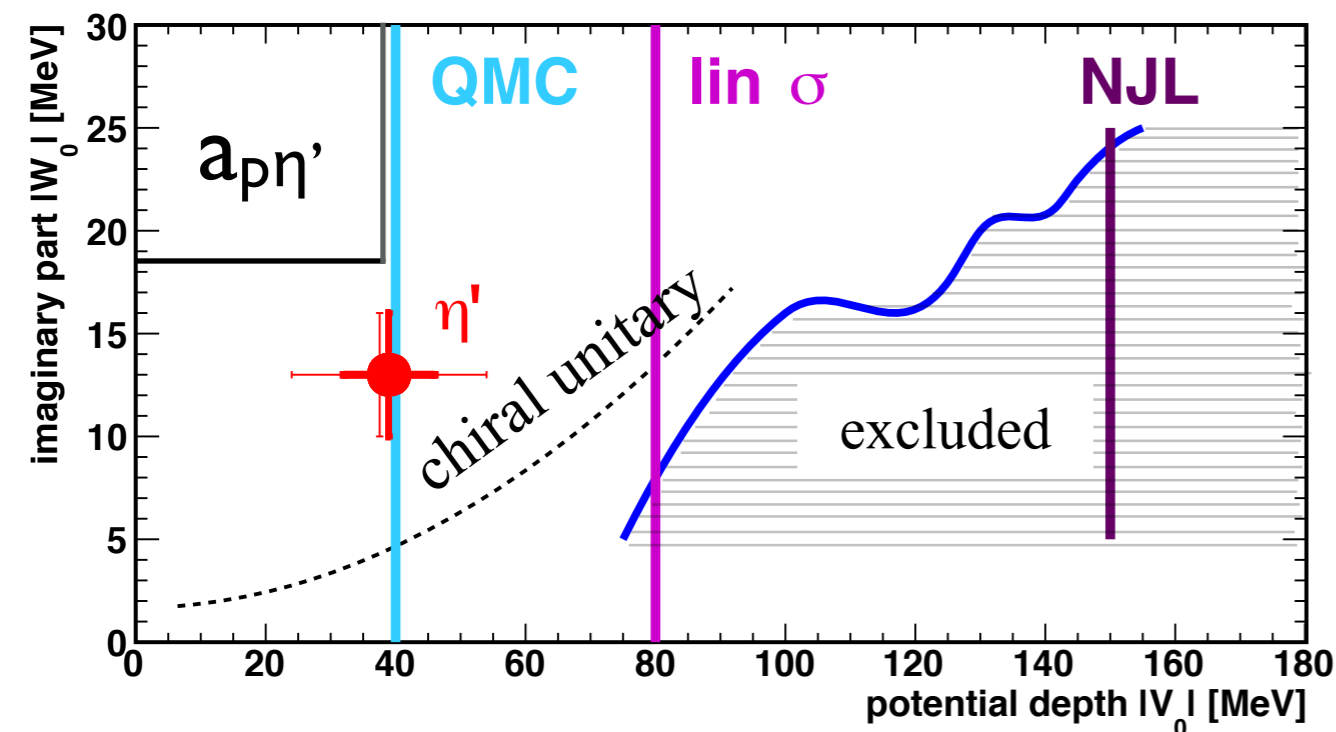
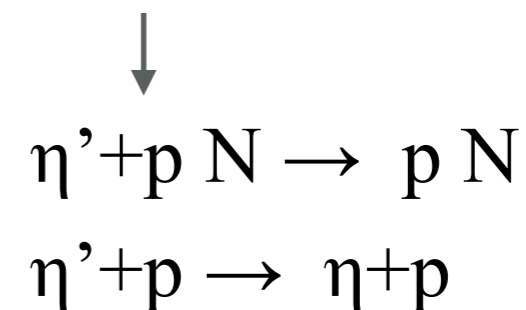
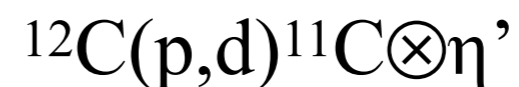
FRS@GSI

Y.K. Tanaka et al., PRL 117 (2016) 202501

Y.K. Tanka et al., PRC 97 (2018) 015202

missing mass spectrometry with  
coincident detection of decay products

K. Itahashi, Y. Tanaka et al., Exp. S 490  
Feb., 2022



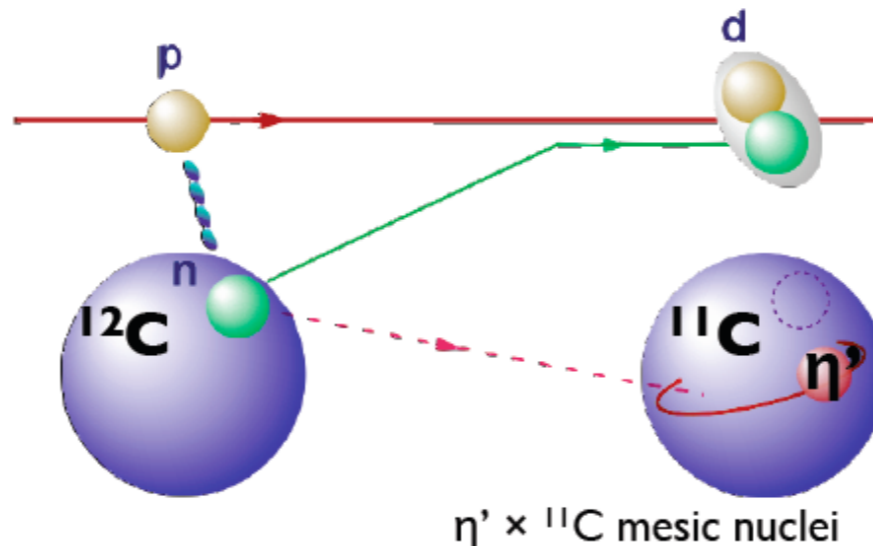
# Search for $\eta'$ - nucleus bound states I

recoilless production in  $^{12}\text{C}(p,d)$  reaction

**PRIME**

collaboration (2012)

K. Itahashi et al., Exp. S 437



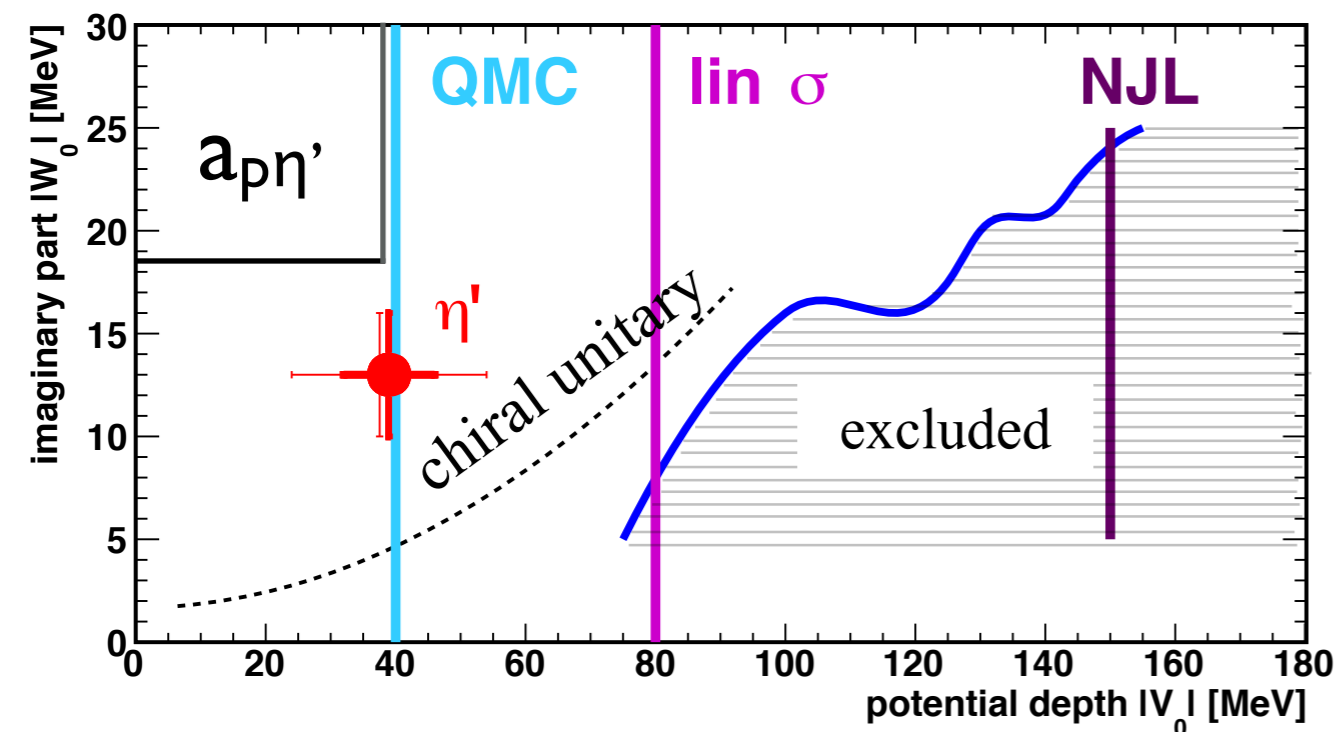
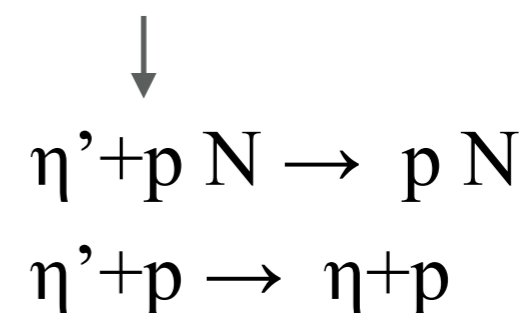
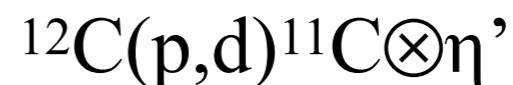
FRS@GSI

Y.K. Tanaka et al., PRL 117 (2016) 202501

Y.K. Tanaka et al., PRC 97 (2018) 015202

missing mass spectrometry with  
coincident detection of decay products

K. Itahashi, Y. Tanaka et al., Exp. S 490  
Feb., 2022

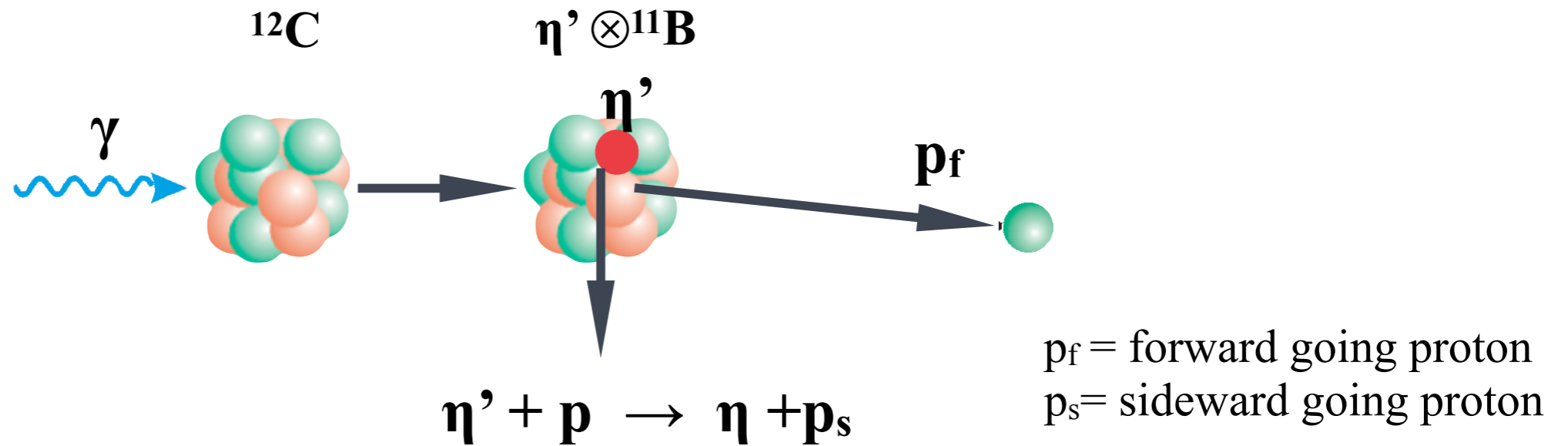


$\Rightarrow$  talk by Y. Tanaka about  $\eta'$ -mesic states

# Search for $\eta'$ - nucleus bound states II

N. Tomida et al. PRL 124 (2020) 202501

LEPS2/BGOegg@Spring-8



missing mass spectrometry with  
coincident detection of decay products

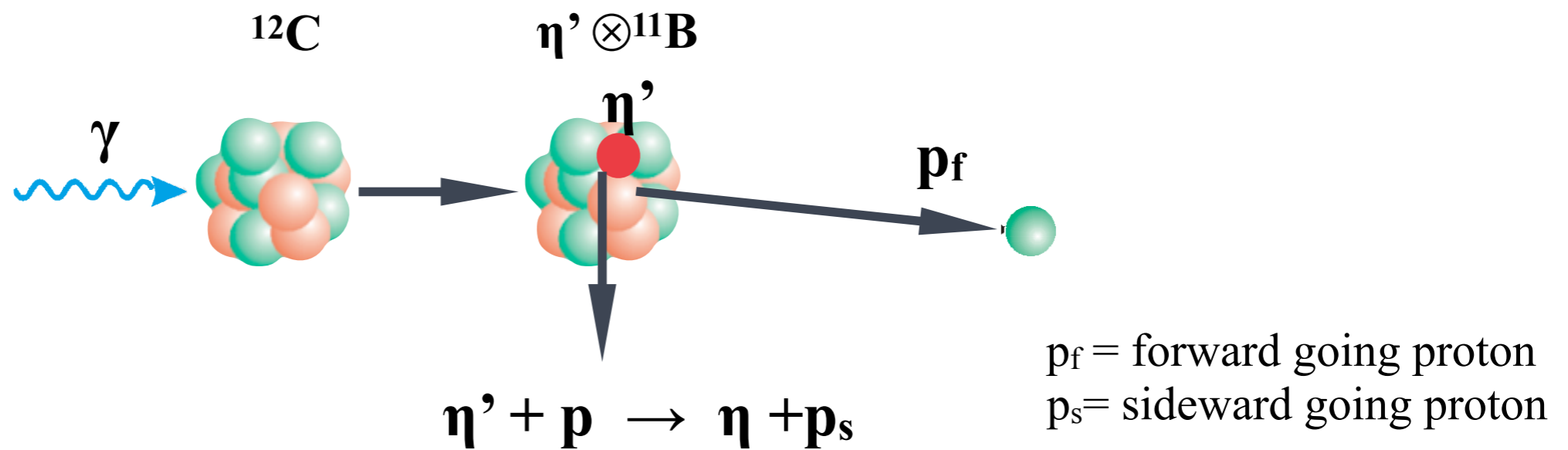
upper limit for branching  
ratio  $\text{BR}(\eta'N \rightarrow \eta N)$   
 $\approx 24\%$  for  $V_0 = -100$  MeV  
 $\approx 80\%$  for  $V_0 = -20$  MeV

$\Rightarrow$  talk by M. Miyabe

# Search for $\eta'$ - nucleus bound states II

N. Tomida et al. PRL 124 (2020) 202501

LEPS2/BGOegg@Spring-8



missing mass spectrometry with  
coincident detection of decay products

upper limit for branching  
ratio  $\text{BR}(\eta'N \rightarrow \eta N)$   
 $\approx 24\%$  for  $V_0 = -100$  MeV  
 $\approx 80\%$  for  $V_0 = -20$  MeV

$\Rightarrow$  talk by M. Miyabe

in both experiments so far only upper limits for production of  $\eta'$  mesic states,  
more to come at this workshop

# Summary & Conclusion

---

meson properties do change in a strongly interacting medium !!

- $\eta'$  is broadened; the lifetime is shortened through inelastic collisions
- large mass modifications  $|\Delta m| > 100$  MeV (as predicted by some calculations) have not been observed
- in-medium effects described within meson-nucleus optical potential

$$V_0 = \Delta m(\rho = \rho_0) = -[39 \pm 7(\text{stat}) \pm 15(\text{syst})] \text{ MeV}$$

$$W_0 = \text{Im } U(\rho = \rho_0, p_{\eta'} \approx 0) = - [13 \pm 3(\text{stat}) \pm 3(\text{syst})] \text{ MeV}$$

**(derived in comparison to model calculations!)**

- the  $\eta'$  meson is a good candidate for forming meson-nucleus bound states since  $|\text{Im } U| \ll |\text{Re } U|$
- search for  $\eta'$  mesic states ongoing; more at this workshop

Backup

# Estimates of the imaginary part of the $\eta'$ -A interaction

---

based on analysis of  $\gamma p \rightarrow p \eta'$  data: SAPHIR, CLAS, CBELSA

$$W = -5 \text{ to } -20 \text{ MeV} \quad \text{H. Nagahiro, M. Takizawa, S. Hirenzaki, PRC 74 (2006) 045203}$$

$$W = -2 \text{ to } -30 \text{ MeV} \quad \text{H. Nagahiro, et al., PLB 709 (2012) 87}$$

based on analysis of  $p p \rightarrow p p \eta'$  data: COSY-11

$$W = -32_{-14}^{+34} \text{ MeV} \quad \text{E. Czerwiński et al., PRL 113 (2014) 062004}$$

theoretical estimate within chiral unitary approach:

$$W \approx -1.8 \text{ MeV} \quad \text{E. Oset and A. Ramos PLB 704 (2011) 334}$$